









Reduced Ice Loss From Greenland Under Stratospheric Aerosol Injection

Special Section:

Modeling in glaciology

 John C. Moore¹ , Ralf Greve^{2,3} , Chao Yue⁴ , Thomas Zwinger⁵ , Fabien Gillet-Chaulet⁶ ,
and Liyun Zhao⁴ 

Key Points:

- Stratospheric aerosol injection at the rate of 5 Tg/yr (G4) lowers Greenland mass loss relative to RCP4.5 by 31%–38% by 2090
- Across four Earth System Model and two ice dynamic models (G4–RCP4.5) differences are 34%–40% in surface mass balance and 16%–34% in ice discharge
- Dynamic mass loss by calving from glaciers is the largest uncertainty between ice dynamics models

Supporting Information:

Supporting Information may be found in the online version of this article.

Correspondence to:

 J. C. Moore,
john.moore.bnu@gmail.com

Citation:

 Moore, J. C., Greve, R., Yue, C., Zwinger, T., Gillet-Chaulet, F., & Zhao, L. (2023). Reduced ice loss from Greenland under stratospheric aerosol injection. *Journal of Geophysical Research: Earth Surface*, 128, e2023JF007112. <https://doi.org/10.1029/2023JF007112>

 Received 19 FEB 2023
 Accepted 31 OCT 2023

Author Contributions:

Conceptualization: John C. Moore, Ralf Greve

Data curation: Ralf Greve

Formal analysis: Ralf Greve, Chao Yue, Thomas Zwinger, Fabien Gillet-Chaulet

Funding acquisition: Ralf Greve

Investigation: Ralf Greve, Thomas Zwinger, Fabien Gillet-Chaulet, Liyun Zhao

Methodology: John C. Moore, Ralf Greve, Chao Yue

© 2023. The Authors.

 This is an open access article under the terms of the [Creative Commons Attribution License](https://creativecommons.org/licenses/by/4.0/), which permits use, distribution and reproduction in any medium, provided the original work is properly cited.

¹Arctic Centre, University of Lapland, Rovaniemi, Finland, ²Institute of Low Temperature Science, Hokkaido University, Sapporo, Japan, ³Arctic Research Center, Hokkaido University, Sapporo, Japan, ⁴State Key Laboratory of Earth Surface Processes and Resource Ecology, Faculty of Geographical Science, Beijing Normal University, Beijing, China, ⁵CSC–IT Center for Science, Espoo, Finland, ⁶Grenoble Alpes University, Grenoble, France

Abstract Sea level rise (SLR) due to surface melt and to dynamic losses from the ice sheets—that is via accelerated flow of glaciers into the sea—is something that may be potentially mitigated by cooling the ice sheet and oceans via solar geoengineering. We use two ice dynamic models driven by changes in surface mass balance (SMB) from four climate models to estimate the SLR contribution from the Greenland ice sheet under the Intergovernmental Panel on Climate Change (IPCC) Representative Concentration Pathway (RCP) 4.5, and 8.5, and Geoengineering Model Intercomparison Project G4 scenarios. The G4 scenario adds 5 Tg/yr sulfate aerosols to the equatorial lower stratosphere (equivalent of 1/4 the 1991 Mt Pinatubo SO₂ eruption) to the IPCC RCP4.5 scenario, which itself approximates the greenhouse gas emission commitments agreed in Paris in 2015. Over the 2020–2090 period, mass loss under G4 is about 31%–38% that under RCP4.5, which is 36%–48% lower than under RCP8.5. Ice lost across the grounding line under both G4 and RCP4.5 is reduced in the future as the termini of many southeast Greenland outlets retreat onto bedrock above sea level. Glaciers with large low-lying catchments in the west, north, and northeast of Greenland (e.g., Jakobshavn, 79N, Zachariae Isstrøm, and Petermann glaciers) discharge more ice from the ice-sheet interior under RCP4.5 than under G4. Although calving losses vary much more than the SMB difference between ice dynamic models, both models point to significant ice discharge losses of between 15% and 42% across the scenarios.

Plain Language Summary Sea level rise from Greenland over the next century may be around 10 cm by 2100. But the amount, and the long-term stability of the ice sheet depend on the degree of summer warming it experiences. Limiting greenhouse gas emissions to the levels pledged by states under the 2015 Paris agreement cuts ice sheet losses by 1/3–1/2 of the losses under the business-as-usual-emissions scenario. If further cooling is induced by aerosols put into the stratosphere at a rate of about 1/4 of the 1991 eruption of Mt Pinatubo, then the ice sheet loss is reduced by about 30% compared with Paris emissions. This specific aerosol geoengineering scenario maintains both the deep and fast-flowing glaciers and the smaller mountain glaciers closer to present sizes than they would be under a greenhouse gas emission scenario similar to international pledges in the 2015 Paris agreement. Iceberg calving remains the most difficult to quantify aspect of Greenland ice loss.

1. Introduction

The Intergovernmental Panel on Climate Change (IPCC) has set targets for limiting damage from climate warming to global mean temperature rises over the 21st century of 1.5°C or 2°C. However, the only internationally agreed consensus on limiting warming is the Nationally Determined Contributions (NDCs) greenhouse gas emissions framework agreed in Paris in 2015. Kitous and Keramidis (2015) note that these NDCs are similar to the trajectory prescribed by the Representative Concentration Pathway (RCP) 4.5 scenario. Global mean temperature rise under RCP4.5 is more likely than not to result in global temperature rise between 2°C and 3°C by 2100 (https://ar5-syr.ipcc.ch/topic_summary.php, Table S1), hence exceeding the 1.5°C and 2°C targets. From the climate simulation perspective, RCP4.5 is close enough to the Paris NDCs that it is a plausibly realistic greenhouse gas scenario that has been widely simulated and on which geoengineering can be added. While RCP8.5 was designed as a “business as usual” scenario prior to the Paris NDC accords, and is hopefully beyond any reasonable emissions agreements, this has also been commonly used as a worst-case scenario. These worst-case scenarios are useful in exploring the “worst that can happen” with climate (Kemp et al., 2022).

Resources: John C. Moore, Ralf Greve, Liyun Zhao
Software: Ralf Greve, Chao Yue, Fabien Gillet-Chaulet
Supervision: John C. Moore, Liyun Zhao
Validation: Ralf Greve, Chao Yue
Visualization: Ralf Greve, Chao Yue, Thomas Zwinger
Writing – original draft: John C. Moore
Writing – review & editing: John C. Moore, Ralf Greve, Chao Yue, Thomas Zwinger, Fabien Gillet-Chaulet, Liyun Zhao

Stratospheric aerosol injection (SAI) has been proposed as a potential method for meeting the IPCC 1.5 or 2°C targets (MacMartin et al., 2018). SAI is a kind of “solar geoengineering” that alters radiative balance and climate by offsetting increases in longwave (LW) absorption by greenhouse gases (GHGs) with reductions in incoming shortwave (SW) solar radiation. A different climate will be produced than experienced in the past with lower GHG LW absorption. This is because, in contrast with GHGs that act 24 hr a day, the spatio-temporal pattern of SW forcing varies daily and seasonally, with the long polar day and night being particularly relevant for ice sheets. Additionally, introducing extraneous material into the atmosphere risks unexpected side effects, and leads to changes in atmospheric chemistry and physical processes (Visoni et al., 2020). The impacts expected under SAI relative to pure GHG force include the reduction of global temperatures, decreased precipitation and humidity, and strengthening of the Atlantic Meridional Ocean Circulation (AMOC, Xie et al., 2022), increased Arctic sea ice (Berdahl et al., 2014), and smaller changes in global teleconnection patterns (Moore et al., 2019; Rezaei et al., 2022). All these elements are crucial for reliable simulation of the ice sheet response to geoengineering scenarios.

Sea level rise (SLR) is one of the chief impacts of rising greenhouse gas emissions (Brown et al., 2021; Hinkel et al., 2014). The SLR contribution from the Greenland ice sheet has been estimated in several different ways. Process-based models driven by greenhouse gas emission scenarios predict a mean SLR of 90 ± 50 and 32 ± 17 mm for RCP8.5 and RCP2.6 respectively relative to a control simulation (Goelzer et al., 2020) by the end of the century. Other methods of estimating the future ice sheet equilibrium geometry produce larger contributions to SLR. Estimating future ice loss by projecting future state of ice sheet imbalance with climate from recent (2000–2019) observations (Box et al., 2022) commits at least 274 ± 68 mm SLR regardless of 21st-century climate pathways although this amount of ice loss will take between 200 and 2,500 years to unfold (see refs in the Box paper). However, there is a considerable risk of higher SLR. For example, if the high-melt year of 2012 is representative of future summers, then an ice loss commitment of 782 ± 135 mm SLR may be eventually expected (Box et al., 2022). A third estimate comes from expert assessment (Bamber & Aspinall, 2013; Oppenheimer et al., 2016), which can be useful because of missing physics in model projections. Year 2100 95% upper-limit SLR ranges from less than 100 mm for a 2°C warming to about 300 mm for a 5°C warming (Jevrejeva et al., 2016). On millennium timescales, Greenland will lose more than 90% of its ice sheet unless summer temperatures are kept to less than 2°C above pre-industrial levels (Pattyn et al., 2018). Changes in downward radiation flux accounted for nearly half of the change in surface mass balance (SMB) during the Eemian period (Van de Berg et al., 2011), and reduced cloud cover over Greenland during the past two decades has been suggested as the most probable cause of accelerated ice sheet mass loss (Hofer et al., 2017). Hence, the Greenland ice sheet is sensitive to both temperature and radiative forcing variability, suggesting it may be especially susceptible to reduced melting by geoengineering.

At present between one third and half the ice sheet mass loss is due to surface melt with the remainder from iceberg calving (Mouginot et al., 2019; Van den Broeke et al., 2009). Much of the ice sheet surface below 2,000 m elevation has suffered accelerating summer melt, which has accelerated since the 1980s as increased summer melt overcame increases in solid precipitation during winter (Van den Broeke et al., 2009).

The calving loss term in the ice sheet mass balance requires ice dynamics models to study—and furthermore depends on both ice sheet basal topography, ocean temperatures, and water circulation within the fjords that channel the waters into contact with the ice sheet. Over time the glaciers draining the ice sheet will be modified, potentially retreating from their present location as ocean and air temperatures warm. Outlets in deeply incised bedrock troughs that extend far inland (Morlighem et al., 2014) are especially vulnerable to ocean forcing and bedrock geometry (Slater et al., 2020). Just a handful of large outlets from the ice sheet have made large contributions to the dynamic mass loss over the observational time frame (Enderlin et al., 2014; McMillan et al., 2016; Mouginot et al., 2019).

The numerical representation of dynamic ice sheet processes related to calving is a notoriously difficult problem as the fundamental process is of discontinuous nature and occurs on far faster timescales (e.g., Åström et al., 2014) than the viscous ice flow that models are mainly concerned with capturing. Therefore, the representation of the brittle-elastic process of calving in continuum-mechanically based ice-sheet models is necessarily a strong simplification. For the Ice Sheet Model Intercomparison Project for CMIP6 (ISMIP6), Goelzer et al. (2020) made use of an empirically derived retreat parameterization for tidewater glaciers (Slater et al., 2019, 2020). Choi et al. (2021) tuned a simple calving parameterization across the ice sheet using observations of velocities at the

calving front. Choi et al. (2021) find that iceberg discharge may account for between 1/3 and 2/3 21st century mass loss, in contrast with other estimates that suggest relatively small calving losses (Aschwanden et al., 2019; Goelzer et al., 2020). Hence, calving constitutes a significant uncertainty factor in estimating Greenland's SLR budget.

The simulation of SMB processes is relatively well understood, and several models have been used with a range of resolutions to explore the response of the ice sheet under various greenhouse gas forcing scenarios (e.g., Goelzer et al., 2020; Pattyn et al., 2018). The SMB is the difference between snow accumulation and surface runoff, and while snowfall may increase under all but the most extreme warming scenarios, the increase in ice ablation rate around the margins is much greater, and enhanced by the altitude feedback mechanism whereby the lowered ice sheet surface is exposed to warmer temperatures. To reliably simulate SMB in a geoengineered climate, a surface energy balance approach must be used that takes into account the altitude feedback, and the differences in radiative forcing caused by the intervention into SW forcing while greenhouse gases raise the longwave forcing.

The evolution of the ice sheet under solar geoengineering has been reported by several studies (Applegate & Keller, 2015; Fettweis et al., 2021; Irvine et al., 2009; Lee et al., 2023). Several of the studies either used a very simple ice sheet model (Applegate & Keller, 2015; Irvine et al., 2009) or neglected ice dynamics (Fettweis et al., 2021). In general, solar geoengineering does slow the ice sheet mass loss rate, but the different GHG and geoengineering scenarios in the various simulations make comparison between them difficult (Irvine et al., 2018). The lack of consistency in climate forcing under solar geoengineering, and in particular for evaluating SAI makes it difficult to establish the robustness of the outcomes.

To address these issues, here we consider scenarios undertaken by multiple climate models, and with scenarios that might be relevant to policy. Models differ in many ways, and no model has been shown to be capable of reliably simulating all the aspects relevant to the ice sheet. Block et al. (2019) illustrated that no single model manages this, even when forced with only GHG emissions. We choose the GeoMIP G4 scenario (Kravitz et al., 2011) because it offers a set of Earth System Models (ESMs) that allows comparison of across-model differences in response. Other SAI scenarios have been studied, exploring reducing RCP8.5 radiative forcing by 50% (Irvine et al., 2019) or to entirely negate RCP8.5 (Tilmes et al., 2018). But these have been performed only by a single ESM to date. The G3 scenario used a variable amount of SAI to balance the time-evolving increase in greenhouse gases under RCP4.5, but was difficult to perform, so was simulated by few models, and has tended to be used as an add-on to G4 (Visioni et al., 2023). More recently the GeoMIP G6 scenario which is designed to reduce radiative forcing from the no-mitigation SSP5-8.5 to the SSP2-4.5 level has been done with a newer generation of climate models, and some output from the SMB change under this forcing has been recently analyzed (Lee et al., 2023), but they have not yet been used to drive any ice dynamics models.

Moore et al. (2019) simulated the Jakobshavn catchment (Guo et al., 2019) with the BISICLES dynamic ice sheet model under G4 SAI, but the whole ice sheet response was not simulated. In this paper we extend the ice dynamics modeling using two different ice dynamical models (Elmer/Ice and SICOPOLIS) to simulate the whole Greenland ice sheet. Furthermore, we show that the ice dynamics used here produce significantly different results for the active Jakobshavn catchment than did BISICLES, and we explore which regions of the ice sheet are most affected by differences in scenario, SMB, and dynamics to the year 2090, when the G4 scenario ends. This article thus builds on the purely SMB induced changes under SAI discussed in Moore et al. (2019) by including the effects of rising oceanic temperatures and associated changes in the marine calving ice sheet outlets.

2. Methods

2.1. Scenarios and Climate Models

The G4 scenario specifies 5 Tg/yr of SO₂ to be injected into the equatorial lower stratosphere for 50 years beginning in 2020. The G4 protocol is unrealistic—it has not yet begun, and multiple injection latitudes with feedback processes would be needed to ensure broad climate targets were met, as envisaged in the Geoengineering Large Ensemble Project simulations (Tilmes et al., 2018). But G4 is moderate in the sense that it could be done relatively cheaply (Smith & Wagner, 2018) compared with costs of damage from GHG forced climate change and perhaps other forms of geoengineering (Moore et al., 2020). The larger the quantities of aerosol placed in the stratosphere, the less effective per kilo is the radiative effect because the aerosols tend to stick to each other and, as they grow, they become less efficient at scattering sunlight (Niemeier & Timmreck, 2015); G4 is expected

Table 1
The Earth System Models Used With Their Equilibrium Climate Sensitivity, and the Shortwave (F_{SRM}) and Net Forcing From the G4 Experiment (Kashimura et al., 2017)

Models	BNU-ESM	HadGEM2-ES	MIROC-ESM	MIROC-ESM-CHEM
Resolution	2.8° × 2.8°	1.25° × 1.875°	2.8° × 2.8°	2.8° × 2.8°
Reference	Ji et al. (2014)	Collins et al. (2011)	Watanabe et al. (2011)	Watanabe et al. (2011)
ECS (K)	3.92 ^a	4.61 ^a	4.42 ^b	4.23 ^b
G4 F_{SRM} (W m ⁻²)	-3.2	-2.5	-1.7	-1.6
G4 net forcing (W m ⁻²)	-1.3	-1.5	-0.4	-0.3

^aSchlund et al. (2020). ^bShingo Watanabe (personal communication, December 12, 2022).

to be radiatively reasonably effective per kilo of injected aerosol. However, since the ESMs all have different sensitivities to CO₂ and sulfate aerosol forcing (Table 1), the constant injection specified by G4 will have varying impacts on radiative balance.

The difference in SW cooling under G4 (Table 1) remains when feedback components of changes in water vapor and cloud forcings are considered, leading to less negative net radiative forcings from G4 SAI with both MIROC model forcings of -0.3 to -0.4 W m⁻² compared with both HadGEM2-ES (-1.5 W m⁻²) and BNU-ESM (-1.3 W m⁻²) (Table 1, Kashimura et al., 2017).

2.2. Bias Correction and Downscaling Climate Forcing

Many studies have forced ice sheet simulations with climate anomalies (e.g., Aschwanden et al., 2019; Goelzer et al., 2013), and a methodology was recently developed under the ISMIP6 collaboration for ice sheet models driven by climate scenarios (S. Nowicki et al., 2020; S. M. J. Nowicki et al., 2016). The ISMIP6 protocol specifies using SMB and surface temperature (ST) anomalies relative to a baseline level over the 1960–1990 period. We differ from the ISMIP6 protocol for ice-sheet–climate simulations (S. Nowicki et al., 2020; S. M. J. Nowicki et al., 2016) in that we use SMB and ST derived from historical simulations of the ESMs over the overlapping period between ISMIP and ERA-Interim (1979–1990). This is because we generate SMB data by driving the SEMIC surface mass and energy balance model (Krapp et al., 2017) with bias corrected ESM forcing fields. SEMIC is a physically based model utilizing an energy-balance approach to compute SMB, runoff and snow-pack properties. SEMIC simulates future changes in ST and SMB (Krapp et al., 2017) in good agreement with the more sophisticated multilayer snowpack model SISVAT included in the regional climate model MAR (Fettweis et al., 2013), and significantly better than simple positive degree schemes (Moore et al., 2019). Moore et al. (2019) built on Krapp et al. (2017) by providing two ways of formulating surface albedo, which is the average of snow albedo and background albedo. One method comes from the Interaction between Soil, Biosphere and Atmosphere (ISBA) model (Douville et al., 1995) and the other uses a different weighting for snow and vegetation. Both surface albedo schemes depend on snow thickness for snow depths lower than 0.45 m. There are also four different snow albedo parameterizations: constant 0.79; melt dependent (Denby et al., 2002); ST gradient-dependent (Slater et al., 1998); and the ISBA parameterization combining melt and snow aging (Douville et al., 1995). These make for eight albedo permutations in total. These eight different parameterizations bracket the MAR estimates in the recent past, and they provide much better estimates of SMB than either the degree day method or the runoff output field from the ESM (Moore et al., 2019). We can also use the spread of the eight parameterizations to estimate the uncertainty in the future SMB for the differences (G4–RCP4.5). We use the same values for all free parameters in SEMIC as Krapp et al. (2017) and use the mean of the eight possible formulations of albedo in the ice dynamics simulations.

We use all ESMs that have daily mean values of incoming SW and LW radiation, ST, surface wind speed, near-surface specific humidity, surface pressure, snowfall and rainfall available for G4, RCP4.5, and RCP8.5 as well as the historical period (Table 1). We calculate air density from near-surface temperature and atmospheric pressure using the ideal gas equation. There are four ESMs that have simulated the G4 experiment and retained data sufficient to run SEMIC and these four ESM model temperature fields were statistically downscaled to 0.5° × 0.5° using an altitude temperature lapse rate of 0.65°C (100 m)⁻¹. Incoming SW and LW radiation, surface

wind speed, near-surface specific humidity, surface pressure, snowfall and rainfall are bi-linearly interpolated into the same $0.5^\circ \times 0.5^\circ$ grid. We bias-corrected the downscaled daily data with Inter-Sectoral Impact Model Intercomparison Project (ISIMIP, Hempel et al., 2013) methods using $0.5^\circ \times 0.5^\circ$ ERA-Interim (Simmons, 2006) from 1979 to 2004 as the observation-based reference climate. Hence, the lapse rate assumption does not affect the agreement between simulation and the reanalysis data. Furthermore, bias correction ensures that model temperatures agree with observations as close as possible—which is particularly important close to the melting point since small biases can lead to large simulated changes in surface albedo and ice sheet mass balance.

This $0.5^\circ \times 0.5^\circ$ resolution is not good enough to resolve individual outlet glaciers, but it is suitable for the atmospheric driving fields, particularly temperature and humidity, which vary on hundred kilometer synoptic scales in the atmosphere. To examine the impact of this forcing at the glacier scale, we need to use detailed topography, which we use to downscale the SEMIC output to the ISMIP6 standard 5 km grid for Greenland (S. Nowicki et al., 2020; S. M. J. Nowicki et al., 2016). Temperature is bi-linearly interpolated to the 5 km grid based on the lapse rate of $0.65^\circ\text{C}/(100\text{ m})$, while SMB is directly bi-linearly interpolated to the 5 km grid, because the overall correlation between SMB and elevation is <0.6 during the historical period. Standard ISMIP6 procedure is to specify an elevation gradient for SMB, but we do not specify an elevation-SMB gradient since we find no significant ($p < 0.05$) trends over the 50-year period of the G4 experiment (Moore et al., 2019), with the linear trends amounting to $8\text{--}20\text{ Gt yr}^{-1}$ in SMB depending on scenario and ESM. This effect may be compared with inter-annual variability in SMB of typically 150 Gt. Instead of an elevation-SMB gradient, here we use the integrated SMB to calculate each year's surface elevation and then estimate the next year's SMB using SEMIC. This procedure does not include dynamic ice flow changes in elevation, but we shall show later that is a small fraction of SMB-driven ice sheet elevation response to the scenarios over the 21st century.

2.3. Ice Dynamics Models

We use two ice sheet dynamic models: SICOPOLIS and Elmer/Ice. SICOPOLIS was set-up as for ISMIP6 projections (Goelzer et al., 2020; Greve et al., 2020), with hybrid “shallow-ice–shelfy-stream” dynamics on grounded ice (Bernales et al., 2017), while floating ice is ignored. Basal sliding under grounded ice is described by a Weertman-Budd-type sliding law with sub-melt sliding and subglacial hydrology (Calov et al., 2018; Kleiner & Humbert, 2014). Geothermal heat flux and paleoclimatic spin-up over 134,000 years until 1990 follow Greve (2019). During the last 9,000 years, the computed topography is continuously nudged toward the (slightly smoothed) observed present-day topography. For the last 9,000 years of the spin-up, the historical run and the future climate simulations, a regular (structured) grid with 5 km resolution is used. In the vertical, we use terrain-following coordinates with 81 layers in the ice domain and 41 layers in the thermal lithosphere layer below. The bed topography is from BedMachine v3 (Morlighem et al., 2017), and glacial isostatic adjustment (GIA) is modeled by the local-lithosphere–relaxing-asthenosphere approach with a time lag of 3,000 years (LeMeur & Huybrechts, 1996). The basal sliding coefficient is determined individually for 20 different regions (Greve et al., 2020) by comparing simulated surface velocities to MEaSUREs v1 observations (Joughin et al., 2016, 2018). The ice front is allowed to move freely. As with the ISMIP6 projections, we impose oceanic forcing via a retreat parameterization for tidewater glaciers, forced by runoff and ocean temperature changes specified for seven ice-ocean sectors around Greenland (Goelzer et al., 2020; Slater et al., 2019, 2020). This parameterization was designed for being used with a wide variety of ice-sheet models, including models like SICOPOLIS that do not resolve smaller outlet glaciers due to the regular grid. We only employ it for the normal, “medium” sensitivity, thereby refraining from exploring the uncertainty of the parameterization via the “high” and “low” sensitivities. Greve et al. (2020) and Greve and Chambers (2022) showed that, while the influence of these different calibrations is notable, it is still smaller than the uncertainty of mass loss due to the different ESM forcings.

The Elmer/Ice (Gagliardini et al., 2013) set-up solves the “shelfy-stream” approximation on a two-dimensional unstructured Finite-Element mesh, containing 195k nodes forming 372k linear triangular elements. The mesh resolution reaches from about 500 m at the outlets to about 50 km in the interior of the ice sheet. The bed topography is from BedMachine v3 (Morlighem et al., 2017), and GIA is ignored. The outline of the domain is kept at the same position, while thinning at shelves as well as grounded ice is allowed to a minimal value. No spin-up is carried out; instead, the 1990 temperature information needed to compute the vertically integrated viscosity is imported from SICOPOLIS results applied in previous full-Stokes simulations (Gillet-Chaulet et al., 2012)—

Table 2

Historical Simulation (*hist*) Taken From the “RCP8.5” Simulation (1990–2015) With MIROC5 (Greve et al., 2020), Control Simulation (*ctrl_proj*), and Future Climate Experiments Discussed in This Study

Period	GCM	Scenario	Ocean forcing	Remark
1990–2015	MIROC5	RCP8.5	—	Historical simulation
2015–2090	—	ctrl_proj	—	Control simulation
2015–2090	BNU-ESM	RCP8.5	Medium	Future climate experiments
2015–2090	HadGEM2-ES	RCP8.5	Medium	
2015–2090	MIROC-ESM	RCP8.5	Medium	
2015–2090	MIROC-ESM-CHEM	RCP8.5	Medium	
2015–2090	BNU-ESM	RCP4.5	Medium	
2015–2090	HadGEM2-ES	RCP4.5	Medium	
2015–2090	MIROC-ESM	RCP4.5	Medium	
2015–2090	MIROC-ESM-CHEM	RCP4.5	Medium	
2015–2090	BNU-ESM	G4	Medium	
2015–2090	HadGEM2-ES	G4	Medium	
2015–2090	MIROC-ESM	G4	Medium	
2015–2090	MIROC-ESM-CHEM	G4	Medium	

Note. Each experiment is carried out with both SICOPOLIS and Elmer/Ice.

so independent of the results obtained within this work. The basal sliding distribution is from data assimilation of MEaSUREs v1 observed surface velocities (Joughin et al., 2016, 2018). Sliding coefficients of the linear Weertman law as well as integrated viscosity distributions are kept constant throughout any of the transient runs. Technically, the ice margin is kept fixed at its present-day location by not allowing the ice thickness to fall below a threshold value of 0.1 m. However, any grid cell for which this threshold is reached is interpreted as ice-free, which in practice allows the ice margin to retreat on top of the—as in the case of SICOPOLIS—forced retreat determined by ISMIP6-type oceanic forcing.

2.4. Model Experiments

We carry out model experiments for all combinations of forcings from the three scenarios RCP8.5, RCP4.5, and G4 and the four ESMs BNU-ESM, HadGEM2-ES, MIROC-ESM, and MIROC-ESM-CHEM from 2015 until 2090. In addition, a control simulation over the same employs a temporally constant climate forcing, using the mean SMB and ST within each model grid cell over the time period 1960–1989 and no oceanic forcing. The 1990–2015 historical simulation bridges the gap between our initialization time 1990 and the CMIP6/ISMIP6 start date of the projections in January 2015. Based on the ISMIP6 recommendation, Greve et al. (2020) and Greve and Chambers (2022) employed a MIROC5/RCP8.5 forcing for this simulation, which we also do here. An overview of the simulations is given in Table 2.

3. Results

3.1. Surface Forcing and SMB

The surface temperatures, from each ESM under each scenario, and SMB anomalies generated by SEMIC when forced by the ESM are shown in Figure 1. Figure S4 of Moore et al. (2019) shows modeled SMB from SEMIC (eight albedo parameterization mean) driven by four ESM ensemble mean climates forcing during 2020–2069 and 2075–2089 under G4, RCP4.5 and RCP8.5 scenarios. Greenland ST rises under G4 are generally 2–3°C higher relative to the 1979–1989 period. Global mean temperature rises are 0.6°C lower during the SAI period

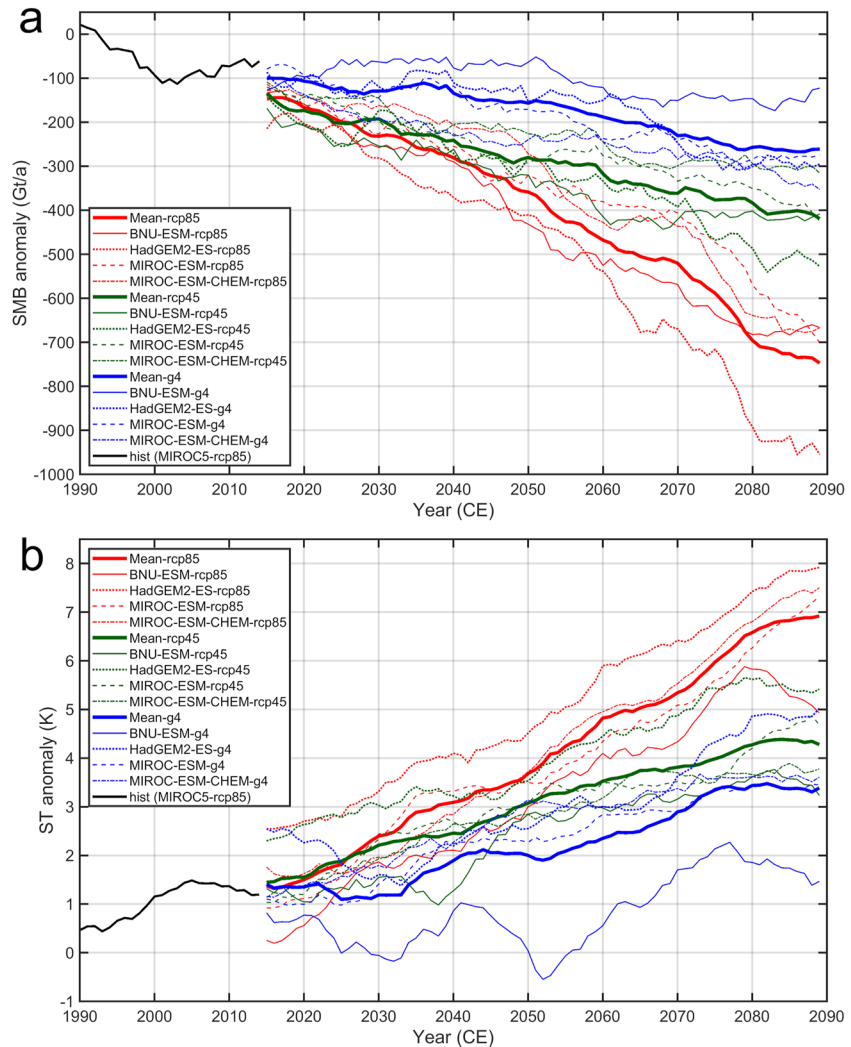


Figure 1. Eleven-year moving averaged anomalies of (a) surface mass balance and (b) surface Greenland air temperature, surface temperature, that drive the ice dynamics models. The anomalies are relative to 1979–1989 (for the historical run [hist] relative to 1960–1989). Labels “XXX-yyy” refer to the Earth System Models (ESMs) and scenarios, “Mean” denotes the four-ESM mean.

(2020–2069) of G4 than for RCP4.5, and those of Greenland are lower by 0.4°C for the MIROC models to 2.2°C for BNU-ESM (Table 3). SMB anomalies become far more negative under all future scenarios, including G4, reflecting the fact that this amount of SAI does not return the state of Greenland to the 20th century norm. Temperature and SMB rises for all models are greater for RCP8.5 than for RCP4.5 and G4, but the across-model spread is similar to the mean differences between scenarios. This is quite typical of the across-model sensitivity to climate forcing (e.g., Block et al., 2019; Goelzer et al., 2020).

3.2. Sea Level Rise

Figure 2 shows how the SLR contribution accumulates under the three climate-change scenarios simulated. The control simulation (“ctrl_proj” in the ISMIP6 terminology; Goelzer et al., 2020) maintains a constant climate forcing throughout the period. For SICOPOLIS, the reference SMB for 1960–1989 was determined by the implied SMB method by Calov et al. (2018) (see also Greve et al. (2020)). This guarantees a small model drift under the control scenario. By contrast, for Elmer/Ice, a similar tuning for stability was not applied; it uses a reference SMB field directly imported from an ESM (MAR3.9-MIROC5) instead. This leads to a rather large model drift toward a growing ice sheet (negative SLR contribution). However, as we use control runs to obtain changes with respect to the drift, this is not a factor that produces different SLR estimates under the different climate forcing scenarios.

Table 3

The Differences (G4–RCP4.5) for Each Earth System Model Having Data Available Over the Greenland Ice Sheet, in Precipitation (PR), Snowfall (SF) in mm Water Equivalent, Downward Shortwave Radiation (SW), Downward Longwave Radiation (LW) SEMIC Surface Mass Balance (Moore et al., 2019), and Over the Whole Earth (T, TOA) During 2020–2069

Models	BNU-ESM	HadGEM2-ES	MIROC-ESM	MIROC-ESM-CHEM	Ensemble
Greenland T (°C)	−2.2	−1.4	−0.5	−0.4	−1.1
Global T (°C)	−0.8	−1.1	−0.4	−0.3	−0.6
PR (mm W.E yr ^{−1})	−16.9	−26.0	−11.2	−9.6	−15.9
SF (mm W.E yr ^{−1})	−5.8	−6.1	1.3	−10.1	−5.2
LW (W m ^{−2})	−8.5	−5.6	−2.3	−1.9	−4.6
SW (W m ^{−2})	−0.2	−0.4	1.2	0.7	0.3
SEMIC SMB (Gt yr ^{−1}) ^a	221 ± 15	155 ± 15	46 ± 15	17 ± 15	114 ± 81
AMOC (Sv)	1.4	0.8	0.4	0.3	0.7
TOA (W/m ²)	−0.5	−0.5	−0.2	−0.2	−0.35
Sept. Sea Ice (10 ⁶ km ²)	0.3	2.4	0.9	0.3	1.0

Note. Also shown are the differences in mean September sea ice extent, AMOC flux and top of atmosphere radiative forcing (TOA) (Xie et al., 2022) for the 2030–2069 period. Differences significant at the 95% are marked in bold according to the signed Wilcoxon rank test. 361.8 Gt of ice will raise global sea levels by 1 mm.

^a±1 standard error in the mean difference ($N = 50$), based on eight SEMIC parameterizations for each ESM.

Relative to the control run (see also Figure 3), by 2090 the SICOPOLIS simulations produce mean (full range) SLR contributions of 90.0 (84.6–96.6) mm for RCP8.5, 60.6 (56.9–63.2) mm for RCP4.5 and 37.6 (22.5–51.8) mm for G4. The corresponding figures for Elmer/Ice are 88.2 mm (79.9–99.8) for RCP8.5, 65.0 (58.3–70.9) mm for RCP4.5 and 44.9 (33.0–56.8) mm for G4. On average across the 12 simulations, Elmer/Ice produces 3.3 mm more SLR than SICOPOLIS, with a root-mean-square deviation of 6.4 mm, and the maximum difference is 10.5 mm (for G4 driven by BNU-ESM). RCP4.5 results overlap with RCP8.5 until about 2050, although RCP8.5 SLRs by MIROC-ESM-CHEM finally become larger than BNU-ESM rises under RCP4.5 only around 2065 with SICOPOLIS or 2078 with ELMER-ICE. The low responsiveness of MIROC models to greenhouse gas forcing in Greenland is not reflected in its relatively high Equilibrium Climate Sensitivity (ECS) (Table 1). But the low response of the MIROC models to SAI (Table 1) and the large response of BNU-ESM (Table 1) are reflected in the much larger differences between G4 and RCP4.5. G4 reduces sea level by 31%–38% on average relative to RCP4.5, with an across model range of 10%–65% and RCP8.5 increases sea level relative to RCP4.5 by 36%–49% (across model range of 25%). See Table S1 for details.

3.3. SLR Components

At present, about half of the mass lost is from surface runoff and the other half from dynamic calving (Van den Broeke et al., 2009). Figure 3 illustrates how the contributions change in the future. SMB changes are almost entirely due to surface melt; changes in snowfall across all scenarios are minor in comparison (Moore et al., 2019). SMB contributions to SLR from 2015 to 2090 under Elmer/Ice simulations are consistently higher than with SICOPOLIS—by averages of 21 mm under RCP8.5 (20.1–21.2 mm across model range), by 18 mm (16.8–18.3 mm) under RCP4.5 and by 14 mm (11–17 mm) under G4 relative to control. Relative to RCP4.5, G4 reduces future SMB contributions to SLR over the 2015–2090 interval by ESM ensemble means of 40% SICOPOLIS and 34% with Elmer/Ice but with a very large across-ESM range (Table S1). MIROC-ESM-CHEM driven differences are only 10%–11%, while BNU-ESM produces 66%–59% differences. This is of course due to the much larger temperature rise differences (G4–RCP4.5) under BNU-ESM than MIROC-ESM-CHEM (Table 3; Figure 1). SMB differences between RCP4.5 and RCP8.5 are similar (42%–34%) as for the G4 and RCP4.5 differences, with an across model range of 21%–67% and with HadGEM2-ES being the largest.

Calving contributions in the future are smaller than SMB according to both SICOPOLIS and Elmer/Ice. Under G4 calving contributes about 16 mm to SLR over 2015–2090 according to SICOPOLIS (7–26 mm across ESM range), and 8 mm with Elmer/Ice (5–12 mm range). Similarly, small contributions come from BNU-ESM and

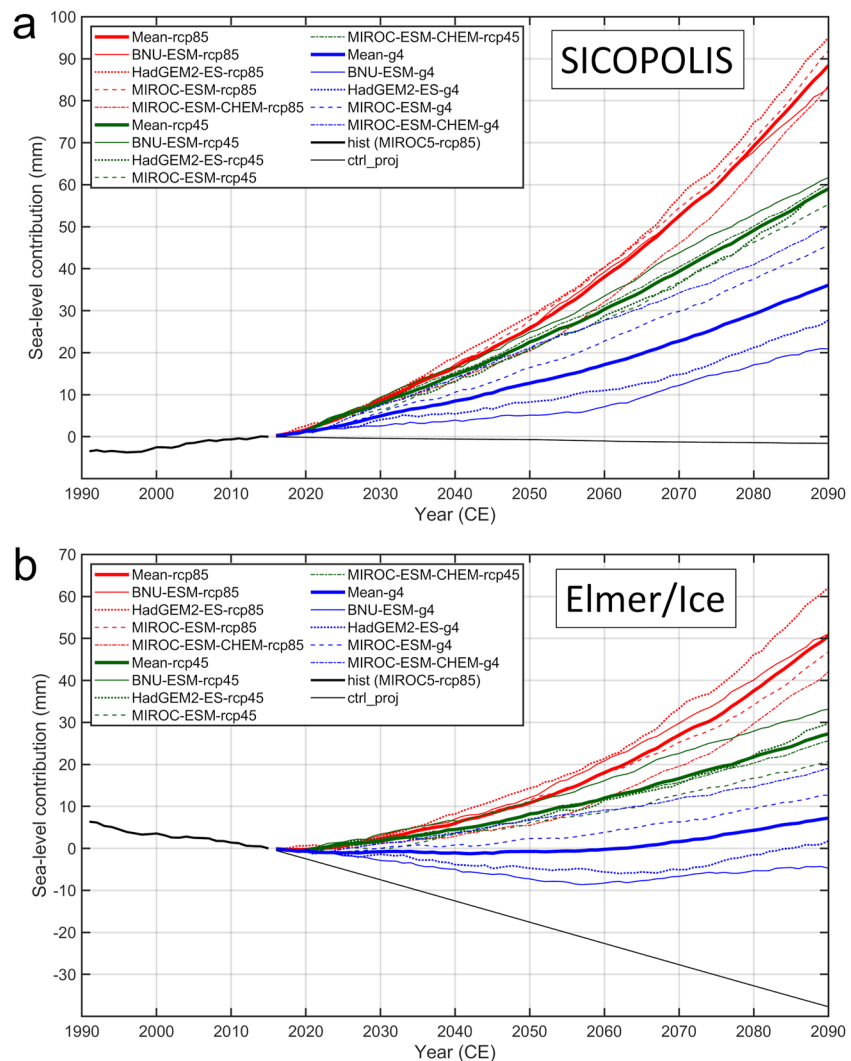


Figure 2. Accumulated sea level equivalent lost by the Greenland ice sheet from (a) SICOPOLIS and (b) Elmer/Ice under the three scenarios with the four Earth System Models (ESMs). The 1990–2015 historical simulation (hist; thick black line) is forced by MIROC5/RCP8.5. The control simulation (ctrl_proj; thin black line) maintains constant forcing throughout. Solid colored (legend) lines are RCP8.5 simulations, dashed for RCP4.5 and dotted curves for G4. Labels “XXX-yyy” refer to the ESMs and scenarios, “Mean” denotes the four-ESM mean.

HadGEM2-ES, with both MIROC models producing larger contributions—by a factor of three with SICOPOLIS. Calving losses under RCP4.5 are only around 16% (4%–39%) larger than those under G4 according to Elmer/Ice while they are around 34% (10%–64%) larger with SICOPOLIS. Calving differences with BNU-ESM are only 4% with Elmer/Ice but 59% with SICOPOLIS; this reflects the very small differences in calving with BNU-ESM driven Elmer/Ice under all three scenarios—from 6.5 to 10.1 mm. RCP8.5 calving is 61% larger than under RCP4.5 with SICOPOLIS and 44% larger with Elmer/Ice. Calving losses driven by both MIROC models are consistently larger than the other two models, reflecting how the MIROC models' smaller rises in ST produce less ice sheet retreat from the margins and so small changes in calving from present than the other two models.

Figures 4–6 compare differences (G4–RCP4.5) between the four ESMs with each of the two ice dynamics models. All four ESM simulations produce larger relative increases in surface lowering along the western margin than along the eastern. MIROC-ESM-CHEM stands out for having smaller SMB differences between G4 and RCP4.5 than the other ESM (Table 3) and relative thickening in the south, that matches the pattern of SMB differences there (cf. Figure S8 of Moore et al. (2019)). The general pattern of SMB may be explained by the combination of ST and specific humidity (or accumulation rate) differences between the models (Moore et al., 2019).

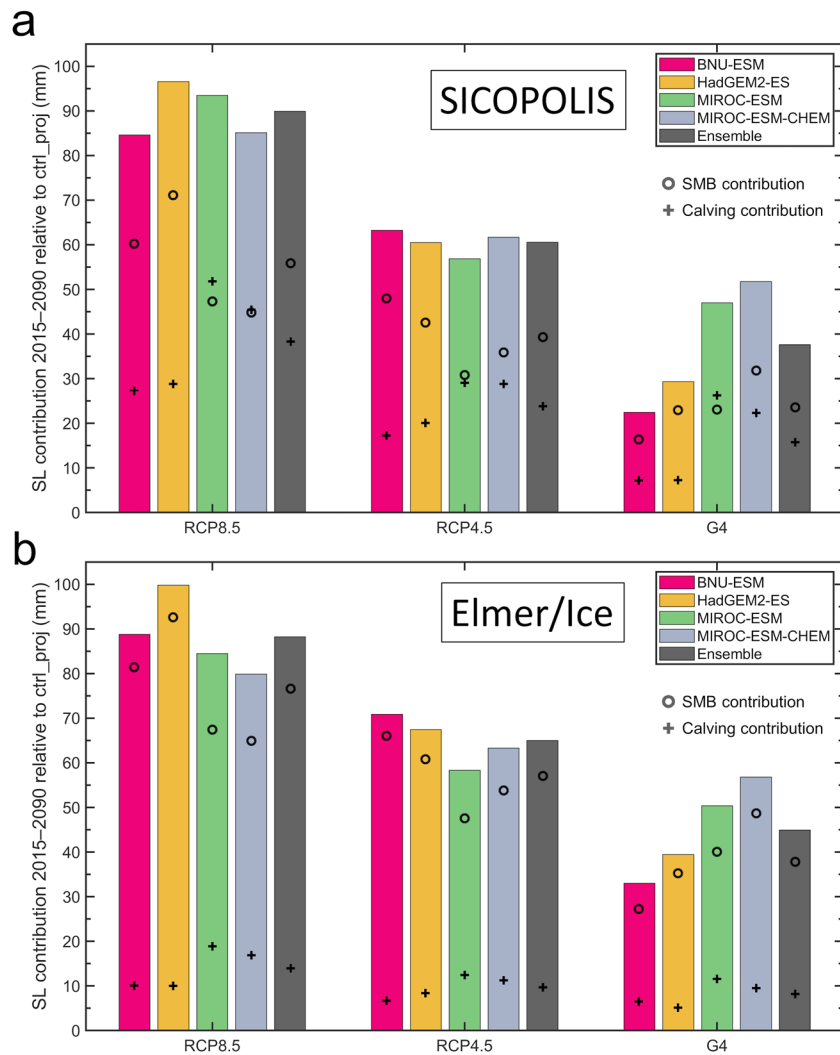


Figure 3. Simulated 2015–2090 change of the ice volume above flotation (colored bars; legend), accumulated surface mass balance (circles) and accumulated calving flux (+markers) from (a) SICOPOLIS and (b) Elmer/Ice. All values are counted positively for ice volume loss and expressed as sea-level contributions relative to the control simulation (ctrl_proj).

Ice flux through the termini of outlet glaciers is lower for the G4 scenario than the RCP4.5 scenario, regardless of climate forcing or ice sheet model. The termini of five dynamically thinning glaciers in Greenland, Kangerlussuaq Glacier in the southeast, Jakobshavn, Upernavik Isstrøm, and Steenstrup glaciers on the western margin, and Zachariae Isstrøm (ZI) in the northeast, contributed more than 12% of the net ice loss during the 4 years from 2011 to 2014 (McMillan et al., 2016). To investigate how these basins respond to different forcings, we look at the change in ice sheet thickness and volume flux. The BNU-ESM simulation shows the largest amplitude range in flux across the various ice sheet basins, especially under Elmer/Ice (Figure 5), but also visibly in Figure 4 for SICOPOLIS. The two MIROC simulations have the smallest ranges, but there are similar spatial patterns in all ESMs (Figures 4 and 5). Figure 6 shows that SICOPOLIS produces larger dynamical differences than Elmer/Ice. Little dynamic differences occur along the east Greenland outlets except for the very active glaciers in the northeast, and in the case of SICOPOLIS, Helheim and Kangerlussuaq glaciers.

The very low-lying termini of the fast-flowing outlets of ZI and Nioghalvfjærdsfjorden (79N) have much greater thinning under RCP4.5 than G4 (Figures 6b and 6d). These two glaciers, along with and Storstrømmen together make up most of the outlets from the North-East Greenland Ice Stream extending up the central ice sheet, that collectively drains 27% of the Greenland ice sheet (Hill et al., 2017). However, the feeder zones higher on the ice sheet show much smaller thinning differences than on the surrounding slow-flowing ice sheet under Elmer/Ice

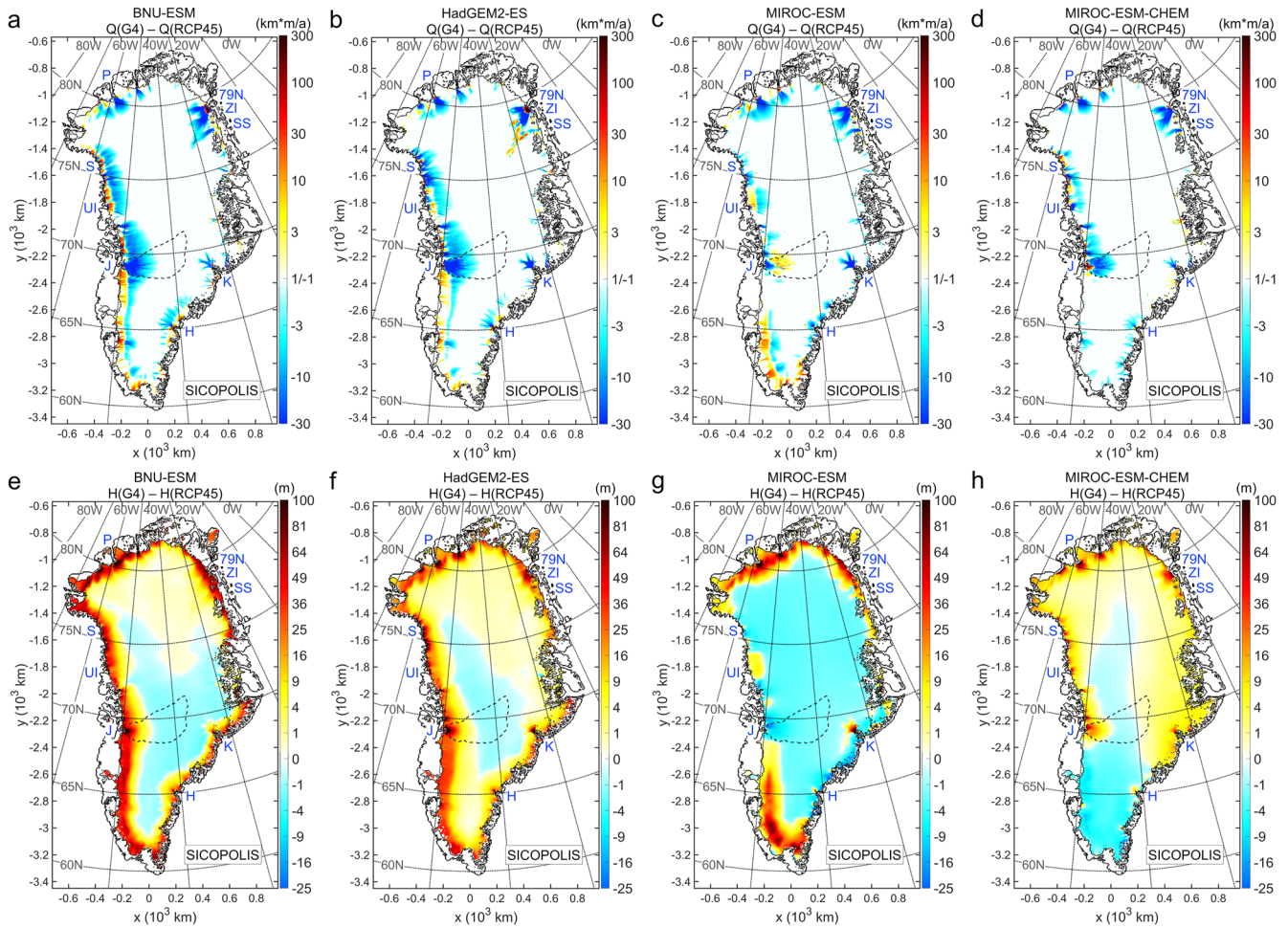


Figure 4. (a–d) G4–RCP4.5 change in volume flux Q (depth-integrated velocity on a positive/negative logarithmic scale), (e–h) G4–RCP4.5 change in ice sheet thickness H (square root scale) in 2090. Results from the four individual Earth System Models ((a, e) BNU-ESM, (b, f) Had-GEM2, (c, g) MIROC-ESM, and (d, h) MIROC-ESM-CHEM) for the SICOPOLIS simulations. Outer (thick) black line: land margin, inner (thin) black line: ice margin in 2015, dashed black line: Jakobshavn drainage basin. Major marine-terminating glaciers: Nioghalvfjærdsfjorden Glacier (79N), Zachariae Isstrøm, Storstrømmen (SS), Kangerlugssuaq Glacier (K), Helheim Glacier (H), Jakobshavn Isbrae (J), Upernavik Isstrøm, Steenstrup Glacier (S), and Petermann Glacier (P).

(Figure 6d), while in SICOPOLIS (Figure 6b) the drainage basin is outlined as a region of small difference in thickness (G4-RCP4.5) in contrast with the surrounding ice sheet, which shows RCP4.5 having thicker ice than under G4 (Figure 6b). Similar patterns are also discernible for the Petermann glacier on the northern coast with relatively small thickness differences above the terminus than the surrounding ice sheet (Figures 6b and 6d). This suggests that the rapid outflow glaciers are being fed by drawing down their interior catchments under RCP4.5 relative to G4. So, as the outlets thin under RCP4.5, there is increased ice flux from inland relative to under G4. This effect is not noticeable in the SICOPOLIS simulations for Jakobshavn nor Kangerlugssuaq glaciers to the south.

The ice flux contrast between glaciers on the west coast north of Jakobshavn and the south-west and east-coasts south of ZI is striking (Figures 6a and 6c). This is in part due to the different topographic control on drainage basins with the eastern and south-western glaciers in mountainous topography (Morlighem et al., 2017). Kangerlugssuaq and Helheim (in the southeast) are susceptible to dynamic losses according to SICOPOLIS (Figure 6a), while there are very small differences in surface elevation change between G4 and RCP4.5 according to Elmer/Ice (Figure 6d). In contrast, glaciers with low-lying hinterlands, such as those in the northeast, north and west, discharge more ice and drain their catchments quicker under RCP4.5 than G4 (Figures 6a and 6c).

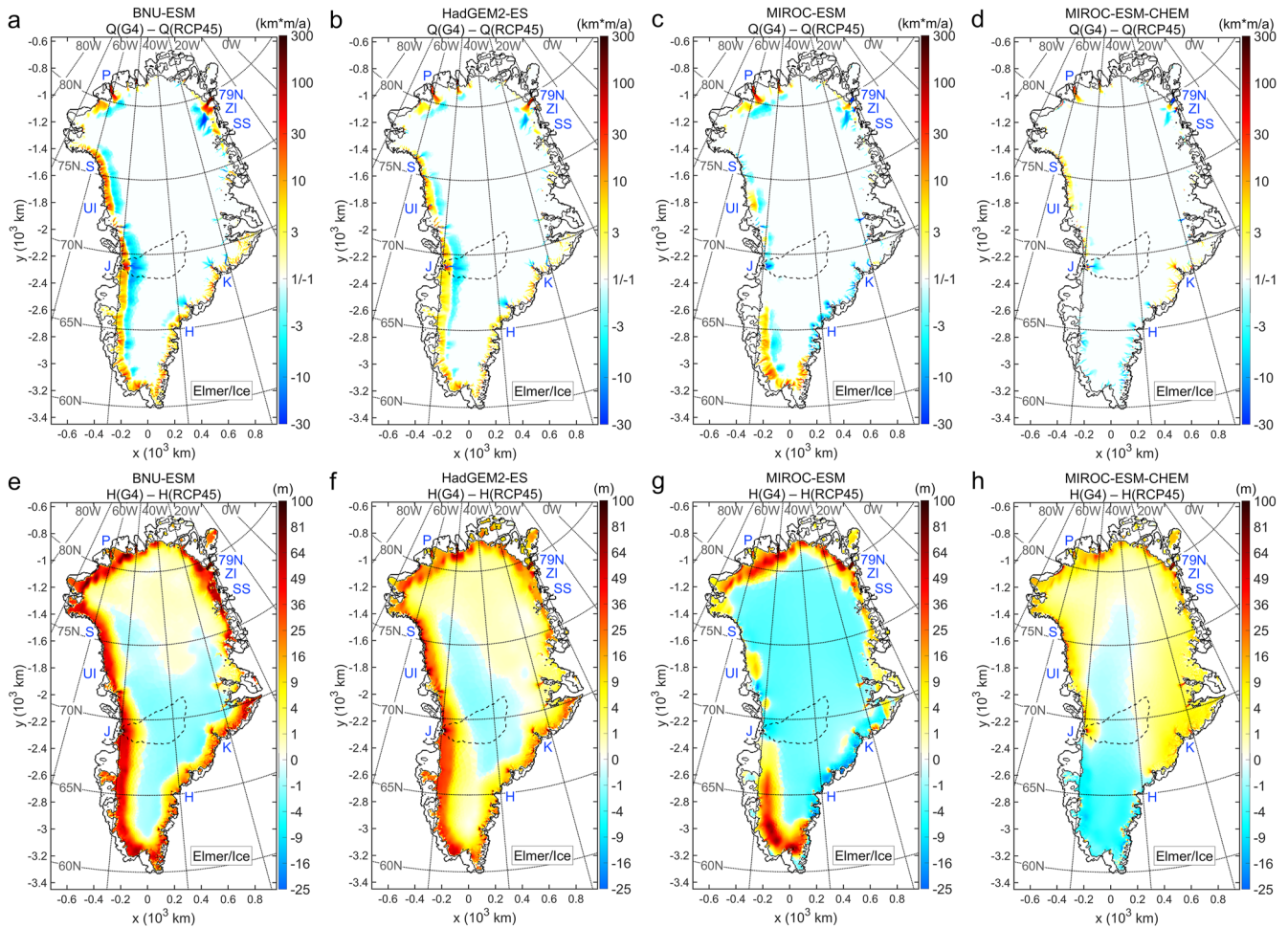


Figure 5. Same as Figure 4 but for the Elmer/Ice simulations.

3.4. Jakobshavn SLR Estimates

We can compare how the different scenarios differ between basins for different ice dynamics models in some detail, and in comparison with the results discussed so far for the whole of Greenland. Moore et al. (2019) applied the BISICLES model, including an active calving formulation, to the Jakobshavn drainage basin of the Greenland ice sheet (as defined by Zwally et al. (2012); holding ~5.3% of the ice sheet's area and ~8% of its mass), and forced it by the same ensemble of ESMs as used here. For this region and the period 2020–2070, they report $15\% \pm 1\%$ less mass loss for G4 relative to RCP4.5. The details of the models in Table 4 show the results from the ice dynamics models applied in this study and the BISICLES model applied in Moore et al. (2019). Elmer/Ice gives smaller differences than SICOPOLIS across all the forcings, as noted earlier for Greenland as a whole. BISICLES estimates are within 35% of the estimates from Elmer/Ice and SICOPOLIS for the BNU-ESM and HadGEM2-ES forcings, but the two MIROC forced simulations have in general far larger differences. The MIROC-ESM model forcing produces a larger mass under RCP4.5 than G4 with SICOPOLIS and Elmer/Ice. This largely accounts for the smaller ensemble mean differences between RCP4.5 and G4 simulated by both Elmer/Ice and SICOPOLIS. There are larger differences between the two MIROC models for the Jakobshavn glacier than seen for the Greenland ice sheet as a whole, which is consistent with models producing more variability on small scales. Figure 4 shows that the behavior of MIROC-ESM-driven ice thickness changes in the Jakobshavn basin are reversed compared with other ESMs, and also contrasting with the nearby outlets, the basin clearly has a greater height under RCP4.5 than G4. Furthermore, this induces a similarly anomalous pattern of mass flux difference, with blue colors dominating the inland basin and red colors near the margin.

The SMB used in all three ice dynamic models comes from the SEMIC simulations driven by the same ESMs and climate scenarios. Therefore, the differences must be due to the ice dynamics models, and particularly the calving

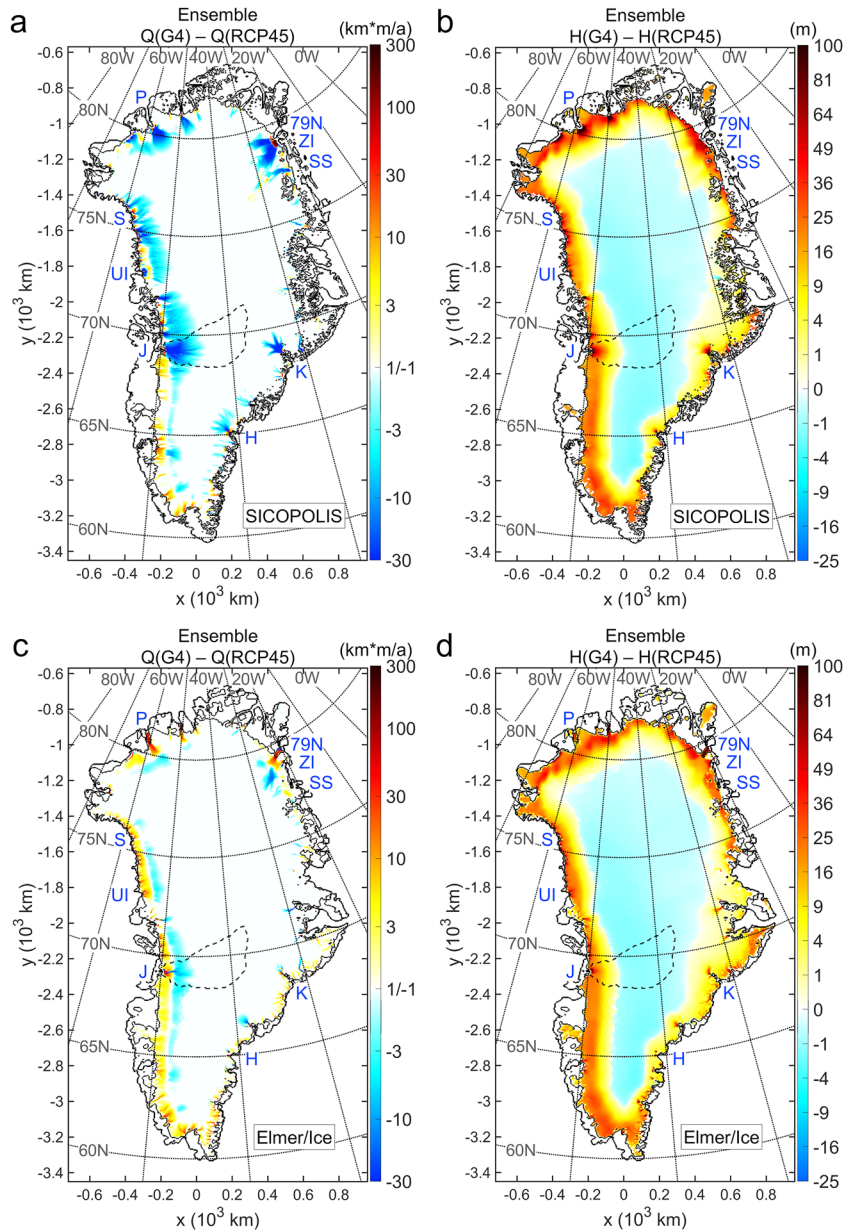


Figure 6. (a, c) G4–RCP4.5 change in volume flux Q (depth-integrated velocity on a positive/negative logarithmic scale), (b, d) G4–RCP4.5 change in ice sheet thickness H (square root scale) in 2090. Four-Earth System Model ensemble means from (a, b) SICOPOLIS and (c, d) Elmer/Ice. Outer (thick) black line: land margin, inner (thin) black line: ice margin in 2015, dashed black line: Jakobshavn drainage basin. Major marine-terminating glaciers: Nioghalvfjerdingsfjorden Glacier (79N), Zachariae Isstrøm, Storstrømmen (SS), Kangerlugssuaq Glacier (K), Helheim Glacier (H), Jakobshavn Isbrae (J), Upernavik Isstrøm, Steenstrup Glacier (S), and Petermann Glacier (P).

Table 4
Mass Change of the Jakobshavn Drainage Basin (G4–RCP4.5) by 2090

Mass change (Gt)	BNU-ESM	HadGEM2-ES	MIROC-ESM	MIROC-ESM-CHEM	Ensemble
Elmer/Ice	+352	+320	−211	+53	+129
SICOPOLIS	+541	+584	−274	+226	+269
BISICLES	+307	+370	+338	+320	+334

parameterized as a function of 300 m ocean temperatures applied by Moore et al. (2019) compared with the ISMIP6-type calving applied here in both SICOPOLIS and Elmer/Ice. The differences for the results driven by the two MIROC models are most striking. This is also visible in the mass flux differences through the Jakobshavn drainage basin in Figures 4 and 5. The modest impact of SAI on SMB in the MIROC simulations (Table 3) leads to rather small changes in SMB between RCP4.5 and G4, and this leads to a positive mass change in the drainage basin with the two ice dynamics models. In contrast, an increase in ocean temperatures leads to increased calving flux in the BISICLES models and corresponding retreat of the glacier (Guo et al., 2019).

4. Discussion

4.1. Differences Due To Forcing

Moore et al. (2019) examined the drivers of SMB change over Greenland under the G4 scenario, especially in the context of changes in the wider Arctic. Although the SW forcing may be expected to be the dominant factor in SMB changes due to the design of the SAI forcing, the study found that the changes in LW forcing affected the SMB. The decline in relative humidity was also critical—since water vapor is an important greenhouse gas—and solar geoengineered climates are inherently drier than pure GHG forced climates (Bala et al., 2008). Change in air-sea heat exchange in the North Atlantic is also a contributing factor to differences under G4 and GHG forcing (Yue et al., 2021). These surface heat flux changes also vary with the advection of heat to the north by the Atlantic Meridional Overturning Circulation (AMOC) that GHG forcing reduces. All types of solar geoengineering act to reverse the decline in GHG-forced AMOC (Xie et al., 2022), helping to maintain heat transport, which hence acts to warm the surface waters around Greenland and modify the reductions in SMB caused by the radiative forcing.

The ESMs differ in a myriad of ways and hence how their responses drive the ice dynamics models (Figures 4 and 5). The key reasons that the four used here produce a spread of differences (RCP4.5–G4) in SMB for Greenland are tabulated in Tables 1 and 3. Fundamental differences are the sensitivities of ESM to greenhouse gas as defined by their ECS and sensitivity to the 5 Tg S/yr SAI forcing (Table 1) and changes in the AMOC that advects heat to Greenland (Table 3). Additionally, the responses driven by SAI and GHG of seasonal sea ice (Table 3), cloud cover, specific humidity and hence longwave radiative absorption and accumulation rates all differ. None of the models stand out among climate models in terms of their climate sensitivities (Schlund et al., 2020). Fundamental differences in SAI forcing compared with pure greenhouse gas scenarios are the designed changes in SW forcing, the induced global drying resulting from changes in temperature lapse rate, and the consequent reductions in humidity and greater transparency of the atmosphere to the outgoing long wave radiation. Another notable difference from greenhouse gas scenarios is the reversal in the declines of AMOC expected with SAI (Xie et al., 2022). Under GHG forcing, the decline in AMOC acts as a negative feedback on ice sheet mass balance as the reduced advection of warmer waters toward the ice sheets offsets some atmospheric warming. The reversal of the AMOC decline (Table 3) seen in all ESM ranging between 0.3 Sv (MIROC-ESM-CHEM) and 1.4 Sv (BNU-ESM) impacts ocean forcing of ice discharge in the ice dynamics models.

A recent analysis of ESM differences in the Arctic across 13 CMIP5 models including BNU-ESM, and MIROC (Block et al., 2019) explains them largely in terms of differing estimates of surface albedo and Planck feedback. The obvious differences in the thickness changes between the two MIROC forced models (Figures 4 and 5), despite them sharing many of the individual model components, show differences in initial conditions (principally Arctic sea ice) and hence natural variability over the 50-year simulations is likely as important as differences due to the model formulation (Block et al., 2019). In addition to these across-model differences in climate, there are likely to be large regions of model simulation space that are unexplored simply because of the single realizations from each ESM, and hence only a small subset of potential “weather” was simulated. Typically, differences in simulations due to differences in the starting state of the climate become less important after about a decade as the natural long-period climate cycles are smoothed (Lehner et al., 2020), so we would expect this to be less important here where we consider multi-decadal integration of ice sheet contributions to SLR.

The two MIROC forced simulations in general behave more like each other than the other models, and they also produce less differences between scenarios and the control. They share many of the same model parameterizations, and so perhaps should not be counted as independent models despite significant differences in their response due to initial conditions. The difference between RCP4.5 and G4 in mass loss amounts to a total of 20 mm (Elmer/Ice) and 23 mm (SICOPOLIS) in mean sea level over the 2015–2090 period. However, trying to

account for the lack of independence in the models by, for example, de-weighting to 75% of the BNU-ESM and HadGEM2-ES ESM makes only 2 mm difference to the ensemble mean results used here, and they are typically assumed to be independent in the ESM literature.

4.2. Comparisons With Other Estimates

Goelzer et al. (2020) used a large ensemble of ice dynamics models with prescribed retreats for the tidewater glaciers driven by RCP8.5 as we use, finding mean SLR contributions at 2100 under RCP8.5 of 90 ± 50 mm. Choi et al. (2021) estimated 79–147 mm from RCP8.5 as simulated by three climate models driving a single ice dynamics model. Both these are very much in line with the RCP8.5 results in Figure 2 (85–96 mm for SICOPOLIS and 80–100 mm for Elmer/Ice), which only extend to 2090. Under G4, about 38–45 mm (ensemble mean for Elmer/Ice and SICOPOLIS simulations, Figure 2) of SLR occurs, which is within the uncertainty of the 32 ± 17 mm that Goelzer et al. (2020) found under RCP2.6. Rückamp et al. (2018) modified RCP2.6 to keep global mean temperatures within 1.5°C of preindustrial (implicitly, by solar geoengineering), finding SLRs lower by 10 mm in 2100 and 17 mm at 2300 relative to RCP2.6.

An analysis of SMB and velocity changes around Greenland from 1972 to 2018 (Mouginot et al., 2019) shows that the majority of mass loss and acceleration were from glaciers draining into the southeastern and northwestern coasts. Little change was recorded in the northern coast outlets or in the southwest. The glaciers in northern Greenland shown as having large changes in ice flux (RCP4.5–G4) in Figure 4 are not the same ones that have registered acceleration from 2000/1 to 2008/9 (Hill et al., 2017); while Humboldt, Petermann and their catchments inland slowed slightly, the outlets from the North-East Greenland Ice Stream accelerated. Hill et al. (2018) showed that continuous retreat into deep fjords at grounded-terminus glaciers led to a greater reduction in basal/lateral resistive stresses and caused high-magnitude acceleration and dynamic thinning.

4.3. Solar Geoengineering and the Arctic

The Brewer-Dobson stratospheric circulation (Butchart, 2014) means that aerosols injected as specified by G4 will be transported poleward. Hence, it is possible that they might be preferentially deposited on the Greenland and Antarctic ice sheets. While SAI aerosols are radiatively active in the stratosphere by design, their radiative effects when deposited on snow will be completely different, and eventually they will form a solution of sulfuric acid. But to put this into context, the anthropogenic SO₂ emissions in the troposphere are about 200 Tg/yr (Aas et al., 2019). These are also transported to the Arctic where they contribute to Arctic haze or atmospheric brown clouds, which also contain black carbon. The black carbon is thought to contribute to surface snow melt even at concentrations of a few parts per billion and the influence of black carbon on temperature and the melting of snow is three times greater than that of CO₂ in Arctic regions (Flanner et al., 2007), although the relative importance of other particles such as dust and ash is greater in many regional snow albedos (e.g., Wang et al., 2022).

Does a global SAI scheme such as G4 or a latitudinal distributed scheme make sense for the conservation of the Greenland ice sheet? There are probably drawbacks to doing global SAI—although the relatively few studies to date have shown that the damage caused by temperature rises outweighs the costs simulated for SAI (Harding et al., 2020). This of course does not mean that all effects of SAI have been examined, and there certainly could be negative consequences. But both the well-established impacts of temperature rises exceeding 2°C, and the risks of unknown consequences as the climate system heats to levels unexplored in the instrumental record are clear already (IPCC, 2018; Kemp et al., 2022). Methods of temperature control that do not address CO₂ concentrations do not tackle its deleterious biogeochemical impacts (Fabry et al., 2008). These will have lasting and damaging consequences for the earth system, but because of the long-term nature of the technology required to decarbonize both industrialized society, and the atmosphere, carbon removal even combined with aggressive emission mitigation will not provide a method for quickly stopping or reversing temperature rises (Vaughan & Lenton, 2011).

Geoengineering is a highly contentious topic. Many have argued that it lacks ethical or governance credibility, even if the challenging engineering needed to perform SAI could be realized (Dannenbergh & Zitzelsberger, 2019). Governance is indeed a key issue, but it is surely the case that all countries would wish to preserve the ice sheets and minimize some of the worst aspects of global heating. Pattyn et al. (2018) showed that the Greenland ice sheet would largely disappear if its summer temperatures warmed by 1.8°C above pre-industrial—although this would take closer to a millennium than a century or two. The feedback between surface lowering and surface

warming means that the longer warming continues, the harder it is to conserve the ice sheet. The Greenland summer temperature rises under G4 are restricted to around 1.6°C, 0.2°C lower than the critical threshold (Pattyn et al., 2018) for long-term irreversible mass loss. Under RCP4.5, our simulations suggest that some outlet glaciers—most notably the North-East Greenland Ice Stream—with long troughs and shallow surface gradients show a dynamic response indicating lowering of the interior of the ice sheet compared with G4; this effect added to lower ocean temperatures under G4 supports the view that G4 SAI would be sufficient to avoid significant ice sheet loss. The present-day ice sheet geometry and behavior are closer to our simulations under G4 than RCP4.5, which opens the possibility that local communities on Greenland may want to employ SAI, or other more targeted ice sheet interventions (Hunt & Byers, 2019), to conserve their lifestyles, fishing, and tourist businesses. The Paris NDC and the RCP4.5 scenarios assume a peak of GHG emissions by the middle of this century. Maintaining global mean temperatures below a 2°C threshold would require about 150 years of SAI, or a century longer than the G4 scenario entails (MacMartin et al., 2018; Rückamp et al., 2018). This would be challenging from a governance perspective given the need for continuous injection and the unprecedented international agreement that would be required.

Other geoengineering schemes may be more palatable, such as SAI focused on the polar regions (Lee et al., 2021)—both Antarctic and Arctic regions would probably have to be treated similarly to preserve hemispheric temperature balance and avoid shifting tropical rainfall patterns (Haywood et al., 2013). From a governance perspective this may simplify the matter but would still be a great challenge as illustrated by the opposition being mounted to small-scale stratospheric micro-physics experiments (<https://www.saamicouncil.net/news-archive/open-letter-requesting-cancellation-of-plans-for-geoengineering>). Injecting into the Arctic stratosphere would also impact climate globally due to equator-ward transport patterns. Certainly, the many indigenous peoples of the North would need early and meaningful consent to any experiments and designs.

Alternative methodologies have been proposed that focus on conserving specific cryosphere components (permafrost: Macias-Fauria et al., 2020; sea ice: Desch et al., 2017; ice sheets: Moore et al., 2018) rather than addressing the mean temperature. These approaches differ in fundamental ways from SAI approaches in that they explicitly seek to preserve the status quo by local or regional interventions rather than modifying the intrinsically global atmosphere. These methods are probably more tractable from ethical and governance perspectives than global solar geoengineering (Moore et al., 2020), but questions on their feasibility remain. In the case of Greenland, where surface melt from the warming atmosphere is likely to be a growing fraction of mass loss as glaciers retreat from the warming oceans, attempts to conserve the ice sheet without addressing surface melt seem to be very difficult. Antarctica, in contrast, is much colder and has very limited surface melt now, and probably over the 21st century (Trusel et al., 2015), making it a better candidate for glacier geoengineering.

5. Conclusions

Here we have shown with two ice dynamics models that solar geoengineering via stratospheric yearly sulfate aerosol injections equivalent to about 1/4 of the 1991 Mt Pinatubo volcanic eruption can reduce mass loss from the Greenland ice sheet compared with the RCP4.5 scenario which matches reasonably well to the greenhouse gas emissions trajectory prescribed in the 2015 Paris NDCs. Greenland's future contributions to SLR are likely to become dominated by atmospheric melt as many glaciers retreat from close contact with oceans. However, this retreat inland may be underestimated in the case of glaciers with deep sub-sea level troughs because the ice dynamics models applied in this study have overly simplified parameterized representations of the calving process. For example, an ice dynamics model designed to match historical calving rates in Jakobshavn, forced with the same climate simulations, predicts much more mass loss than the ice dynamics models without such active calving processes, as does a whole ice sheet model with calving rates tuned to observations (Choi et al., 2021).

Overall mass losses under G4 are about 35% lower than under RCP4.5. The two ice dynamics models used here differ in estimates of SMB by much smaller amounts (34%–40%) than they differ in the ice discharge differences (16%–34%). This implies that improvement in the physics of the ice dynamics models, such as better representation of the calving process, would be worth pursuing—even in the case of Greenland which has much smaller calving fluxes than Antarctica.

Finally, we emphasize that the aim of this paper is not to promote the deployment of SAI-type geoengineering. Any wider consideration of geoengineering approaches must always take into account the conceivable adverse

effects as well. Geoengineering only deals with the symptoms, rather than tackling the root cause of climate change, and it may even serve as an excuse for avoiding or delaying the fundamental societal changes required to consequently limit greenhouse-gas emissions. Further, even if the net impact of any intervention is positive, in a complex system like the Earth it is likely that adverse side effects will hit people who have not demanded it. Therefore, we keep a neutral stance and merely wish to contribute to the discussion by adding our piece of information that the decay of the Greenland ice sheet can be slowed down under the G4 scenario compared to RCP4.5.

Data Availability Statement

SICOPOLIS and Elmer/Ice are free and open-source software, published on Zenodo (SICOPOLIS Authors, 2022, <https://doi.org/10.5281/zenodo.8084818>; Elmer/Ice Authors, 2022, <https://doi.org/10.5281/zenodo.7892181>). Scripts related to the ISMIP-method downscaling, SEMIC code, as well as configuration files, input files, and model output from SICOPOLIS and Elmer/Ice are archived on Zenodo (Moore et al., 2023, <https://doi.org/10.5281/zenodo.4131582>). GeoMIP and CMIP5 data are available on the Earth System Grid Federation (ESGF) data nodes (CMIP5 Contributors, 2014; GeoMIP Contributors, 2013).

Acknowledgments

We thank Heiko Goelzer (NORCE Norwegian Research Centre, Bjerknes Centre for Climate Research, Bergen, Norway) for his support with adding the ISMIP6-type oceanic forcing to our simulations, and the scientists managing the Earth System Grid Federation (ESGF) who have assisted with making GeoMIP output available. We also thank the Editor Olga Sergienko, the Associate Editor, and three reviewers for constructive remarks and suggestions that helped to improve the manuscript. This study is supported by the National Key Research and Development Program of China (2021YFB3900105), State Key Laboratory of Earth Surface Processes and Resource Ecology (2022-ZD-05), Finnish Academy COLD consortium Grants 322430 and 322978, Japan Society for the Promotion of Science (JSPS) KAKENHI Grant JP16H02224 and JP17H06104, Arctic Challenge for Sustainability projects (ArCS, ArCS II) of the Japanese MEXT (program Grant JPMXD1300000000 and JPMXD1420318865), and a Hokkaido University Foreign Visiting Professorship at the Institute of Low Temperature Science.

References

- Aas, W., Mortier, A., Bowersox, V., Cherian, R., Faluvegi, G., Fagerli, H., et al. (2019). Global and regional trends of atmospheric sulfur. *Scientific Reports*, 9(1), 953. <https://doi.org/10.1038/s41598-018-37304-0>
- Applegate, P. J., & Keller, K. (2015). How effective is albedo modification (solar radiation management geoengineering) in preventing sea-level rise from the Greenland Ice Sheet? *Environmental Research Letters*, 10(8), 084018. <https://doi.org/10.1088/1748-9326/10/8/084018>
- Aschwanden, A., Fahnestock, M. A., Truffer, M., Brinkerhoff, D. J., Hock, R., Khroulev, C., et al. (2019). Contribution of the Greenland Ice Sheet to sea level over the next millennium. *Science Advances*, 5(6), eaav9396. <https://doi.org/10.1126/sciadv.aav9396>
- Åström, J. A., Vallot, D., Schäfer, M., Welty, E. Z., O'Neel, S., Bartholomäus, T. C., et al. (2014). Termini of calving glaciers as self-organised critical systems. *Nature Geoscience*, 7(12), 874–878. <https://doi.org/10.1038/ngeo2290>
- Bala, G., Duffy, P. B., & Taylor, K. E. (2008). Impact of geoengineering schemes on the global hydrological cycle. *Proceedings of the National Academy of Sciences of the United States of America*, 105(22), 7664–7669. <https://doi.org/10.1073/pnas.0711648105>
- Bamber, J. L., & Aspinall, W. (2013). An expert judgement assessment of future sea level rise from the ice sheets. *Nature Climate Change*, 3(4), 424–427. <https://doi.org/10.1038/nclimate1778>
- Berdahl, M., Robock, A., Ji, D., Moore, J. C., Jones, A., Kravitz, B., & Watanabe, S. (2014). Arctic cryosphere response in the geoengineering model intercomparison project (GeoMIP) G3 and G4 scenarios. *Journal of Geophysical Research: Atmospheres*, 119(3), 1308–1321. <https://doi.org/10.1002/2013JD020627>
- Bernales, J., Rogozhina, I., Greve, R., & Thomas, M. (2017). Comparison of hybrid schemes for the combination of shallow approximations in numerical simulations of the Antarctic Ice Sheet. *The Cryosphere*, 11(1), 247–265. <https://doi.org/10.5194/tc-11-247-2017>
- Block, K., Schneider, F. A., Mühlensstädt, J., Salzmann, M., & Quaas, J. (2019). Climate models disagree on the sign of total radiative feedback in the Arctic. *Tellus A: Dynamic Meteorology and Oceanography*, 72(1), 1–14. <https://doi.org/10.1080/16000870.2019.1696139>
- Box, J. E., Hubbard, A., Bahr, D. B., Colgan, W. T., Fettweis, X., Mankoff, K. D., et al. (2022). Greenland ice sheet climate disequilibrium and committed sea-level rise. *Nature Climate Change*, 12(9), 808–813. <https://doi.org/10.1038/s41558-022-01441-2>
- Brown, S., Jenkins, K., Goodwin, P., Lincke, D., Vafeidis, A. T., Tol, R. S. J., et al. (2021). Global costs of protecting against sea-level rise at 1.5 to 4.0°C. *Climatic Change*, 167(1–2), 4. <https://doi.org/10.1007/s10584-021-03130-z>
- Butchart, N. (2014). The Brewer-Dobson circulation. *Reviews of Geophysics*, 52(2), 157–184. <https://doi.org/10.1002/2013RG000448>
- Calov, R., Beyer, S., Greve, R., Beckmann, J., Willeit, M., Kleiner, T., et al. (2018). Simulation of the future sea level contribution of Greenland with a new glacial system model. *The Cryosphere*, 12(10), 3097–3121. <https://doi.org/10.5194/tc-12-3097-2018>
- Choi, Y., Morlighem, M., Rignot, E., & Wood, M. (2021). Ice dynamics will remain a primary driver of Greenland ice sheet mass loss over the next century. *Communications Earth & Environment*, 2(1), 26. <https://doi.org/10.1038/s43247-021-00092-z>
- CMIP5 Contributors. (2014). Coupled model intercomparison project 5 (CMIP5) [Dataset]. Earth System Grid Federation (ESGF). Retrieved from <https://esgf-node.llnl.gov/projects/cmip5/>
- Collins, W. J., Bellouin, N., Doutriaux-Boucher, M., Gedney, N., Halloran, P., Hinton, T., et al. (2011). Development and evaluation of an earth-system model – HadGEM2. *Geoscientific Model Development*, 4, 1051–1075. <https://doi.org/10.5194/gmd-4-1051-2011>
- Dannenberg, A., & Zitzelsberger, S. (2019). Climate experts' views on geoengineering depend on their beliefs about climate change impacts. *Nature Climate Change*, 9(10), 769–775. <https://doi.org/10.1038/s41558-019-0564-z>
- Denby, B., Greuell, W., & Oerlemans, J. (2002). Simulating the Greenland atmospheric boundary layer Part I: Model description and validation. *Tellus*, 54(5), 512–528. <https://doi.org/10.3402/tellusa.v54i5.12170>
- Desch, S. J., Smith, N., Groppi, C., Vargas, P., Jackson, R., Kalyaan, A., et al. (2017). Arctic ice management. *Earth's Future*, 5(1), 107–127. <https://doi.org/10.1002/2016EF000410>
- Douville, H., Royer, J. F., & Mahfouf, J. (1995). A new snow parameterization for the Météo-France climate model. *Climate Dynamics*, 12(1), 21–35. <https://doi.org/10.1007/BF00208760>
- Elmer/Ice Authors. (2022). Elmer/Ice (version 9.0, branch devel, revision 9cbac68b3) [Software]. Zenodo. <https://doi.org/10.5281/zenodo.7892181>
- Enderlin, E. M., Howat, I. M., Jeong, S., Noh, M.-J., van Angelen, J. H., & van den Broeke, M. R. (2014). An improved mass budget for the Greenland ice sheet. *Geophysical Research Letters*, 41(3), 866–872. <https://doi.org/10.1002/2013GL059010>
- Fabry, V. J., Seibel, B. A., Feely, R. A., & Orr, J. C. (2008). Impacts of ocean acidification on marine fauna and ecosystem processes. *ICES Journal of Marine Science*, 65(3), 414–432. <https://doi.org/10.1093/icesjms/fsn048>
- Fettweis, X., Franco, B., Tedesco, M., van Angelen, J. H., Lenaerts, J. T. M., van den Broeke, M. R., & Gallée, H. (2013). Estimating the Greenland ice sheet surface mass balance contribution to future sea level rise using the regional atmospheric climate model MAR. *The Cryosphere*, 7(2), 469–489. <https://doi.org/10.5194/tc-7-469-2013>

- Fettweis, X., Hofer, S., Séférian, R., Amory, C., Delhasse, A., Doutreloup, S., et al. (2021). Brief communication: Reduction in the future Greenland ice sheet surface melt with the help of solar geoengineering. *The Cryosphere*, 15(6), 3013–3019. <https://doi.org/10.5194/tc-15-3013-2021>
- Flanner, M. G., Zender, C. S., Randerson, J. T., & Rasch, P. J. (2007). Present-day climate forcing and response from black carbon in snow. *Journal of Geophysical Research*, 112(D11), D11202. <https://doi.org/10.1029/2006JD008003>
- Gagliardini, O., Zwinger, T., Gillet-Chaulet, F., Durand, G., Favier, L., de Fleurian, B., et al. (2013). Capabilities and performance of Elmer/Ice, a new-generation ice sheet model. *Geoscientific Model Development*, 6(4), 1299–1318. <https://doi.org/10.5194/gmd-6-1299-2013>
- GeoMIP Contributors. (2013). The geoenvironmental model intercomparison project (GeoMIP) [Dataset]. Earth System Grid Federation (ESGF). Retrieved from <https://esgf-node.llnl.gov/search/esgf-llnl/>
- Gillet-Chaulet, F., Gagliardini, O., Seddik, H., Nodet, M., Durand, G., Ritz, C., et al. (2012). Greenland ice sheet contribution to sea-level rise from a new-generation ice-sheet model. *The Cryosphere*, 6(6), 1561–1576. <https://doi.org/10.5194/tc-6-1561-2012>
- Goelzer, H., Huybrechts, P., Fürst, J., Nick, F., Andersen, M., Edwards, T. L., et al. (2013). Sensitivity of Greenland ice sheet projections to model formulations. *Journal of Glaciology*, 59(216), 733–749. <https://doi.org/10.3189/2013JG121182>
- Goelzer, H., Nowicki, S., Payne, A., Larour, E., Seroussi, H., Lipscomb, W. H., et al. (2020). The future sea-level contribution of the Greenland ice sheet: A multi-model ensemble study of ISMIP6. *The Cryosphere*, 14(9), 3071–3096. <https://doi.org/10.5194/tc-14-3071-2020>
- Greve, R. (2019). Geothermal heat flux distribution for the Greenland ice sheet, derived by combining a global representation and information from deep ice cores. *Polar Data Journal*, 3, 22–36. <https://doi.org/10.20575/00000006>
- Greve, R., & Chambers, C. (2022). Mass loss of the Greenland ice sheet until the year 3000 under a sustained late-21st-century climate. *Journal of Glaciology*, 68(269), 618–624. <https://doi.org/10.1017/jog.2022.9>
- Greve, R., Chambers, C., & Calov, R. (2020). ISMIP6 future projections for the Greenland ice sheet with the model SICOPOLIS. *Zenodo*. <https://doi.org/10.5281/zenodo.3971251>
- Guo, X., Zhao, L., Gladstone, R., Sun, S., & Moore, J. C. (2019). Simulated retreat of Jakobshavn Isbræ during the 21st century. *The Cryosphere*, 13(11), 3139–3153. <https://doi.org/10.5194/tc-13-3139-2019>
- Harding, A. R., Ricke, K., Heyen, D., Macmartin, D. G., & Moreno-Cruz, J. (2020). Climate econometric models indicate solar geoengineering would reduce inter-country income inequality. *Nature Communications*, 11(1), 227. <https://doi.org/10.1038/s41467-019-13957-x>
- Haywood, J., Jones, A., Bellouin, N., & Stephenson, D. (2013). Asymmetric forcing from stratospheric aerosols impacts Sahelian rainfall. *Nature Climate Change*, 3(7), 660–665. <https://doi.org/10.1038/nclimate1857>
- Hempel, S., Frieler, K., Warszawski, L., Schewe, J., & Piontek, F. (2013). A trend-preserving bias correction – The ISI-MIP approach. *Earth System Dynamics*, 4(2), 219–236. <https://doi.org/10.5194/esd-4-219-2013>
- Hill, E. A., Carr, J. R., & Stokes, C. R. (2017). A review of recent changes in major marine-terminating outlet glaciers in northern Greenland. *Frontiers in Earth Science*, 4, 111. <https://doi.org/10.3389/feart.2016.00111>
- Hill, E. A., Carr, J. R., Stokes, C. R., & Gudmundsson, G. H. (2018). Dynamic changes in outlet glaciers in northern Greenland from 1948 to 2015. *The Cryosphere*, 12(10), 3243–3263. <https://doi.org/10.5194/tc-12-3243-2018>
- Hinkel, J., Lincke, D., Vafeidis, A. T., Perrette, M., Nicholls, R. J., Tol, R. S. J., et al. (2014). Coastal flood damage and adaptation costs under 21st century sea-level rise. *Proceedings of the National Academy of Sciences of the United States of America*, 111(9), 3292–3297. <https://doi.org/10.1073/pnas.1222469111>
- Hofer, S., Tedstone, A. J., Fettweis, X., & Bamber, J. L. (2017). Decreasing cloud cover drives the recent mass loss on the Greenland ice sheet. *Science Advances*, 3(6), e1700584. <https://doi.org/10.1126/sciadv.1700584>
- Hunt, J. D., & Byers, E. (2019). Reducing sea level rise with submerged barriers and dams in Greenland. *Mitigation and Adaptation Strategies for Global Change*, 24(5), 779–794. <https://doi.org/10.1007/s11027-018-9831-y>
- IPCC. (2018). Global Warming of 1.5°C. An IPCC Special Report on the impacts of global warming of 1.5°C above pre-industrial levels and related global greenhouse gas emission pathway. In V. Masson-Delmotte, P. Zhai, H.-O. Pörtner, D. Roberts, J. Skea, A. Shukla, et al. (Eds.), *The context of strengthening the global response to the threat of climate change, sustainable development, and efforts to eradicate poverty* (p. 616). Cambridge University Press. <https://doi.org/10.1017/9781009157940>
- Irvine, P. J., Emanuel, K., He, J., Horowitz, L. W., Vecchi, G., & Keith, D. (2019). Halving warming with idealized solar geoengineering moderates key climate hazards. *Nature Climate Change*, 9(4), 295–299. <https://doi.org/10.1038/s41558-019-0398-8>
- Irvine, P. J., Keith, D. W., & Moore, J. (2018). Brief communication: Understanding solar geoengineering's potential to limit sea level rise requires attention from cryosphere experts. *The Cryosphere*, 12(7), 2501–2513. <https://doi.org/10.5194/tc-12-2501-2018>
- Irvine, P. J., Lunt, D. J., Stone, E. J., & Ridgwell, A. J. (2009). The fate of the Greenland ice sheet in a geoengineered, high CO₂ world. *Environmental Research Letters*, 4(4), 045109. <https://doi.org/10.1088/1748-9326/4/4/045109>
- Jevrejeva, S., Jackson, L. P., Riva, R. E. M., Grinsted, A., & Moore, J. C. (2016). Coastal sea level rise with warming above 2°C. *Proceedings of the National Academy of Sciences of the United States of America*, 113(47), 13342–13347. <https://doi.org/10.1073/pnas.1605312113>
- Ji, D., Wang, L., Feng, J., Wu, Q., Cheng, H., Zhang, Q., et al. (2014). Description and basic evaluation of Beijing Normal University earth system model (BNU-ESM) version 1. *Geoscientific Model Development*, 7(5), 2039–2064. <https://doi.org/10.5194/gmd-7-2039-2014>
- Joughin, I., Smith, B. E., & Howat, I. M. (2018). A complete map of Greenland ice velocity derived from satellite data collected over 20 years. *Journal of Glaciology*, 64(243), 1–11. <https://doi.org/10.1017/jog.2017.73>
- Joughin, I., Smith, B. E., Howat, I. M., & Scambos, T. (2016). MEaSUREs multi-year Greenland ice sheet velocity mosaic, version 1 [Dataset]. NASA National Snow and Ice Data Center Distributed Active Archive Center. <https://doi.org/10.5067/QUA5Q9SVMSJG>
- Kashimura, H., Abe, M., Watanabe, S., Sekiya, T., Ji, D., Moore, J. C., et al. (2017). Shortwave radiative forcing, rapid adjustment, and feedback to the surface by sulfate geoengineering: Analysis of the geoengineering model intercomparison project G4 scenario. *Atmospheric Chemistry and Physics*, 17(5), 3339–3356. <https://doi.org/10.5194/acp-17-3339-2017>
- Kemp, L., Xu, C., Depledge, J., Ebi, K. L., Gibbins, G., Kohler, T. A., et al. (2022). Climate Endgame: Exploring catastrophic climate change scenarios. *Proceedings of the National Academy of Sciences of the United States of America*, 119(34), e2108146119. <https://doi.org/10.1073/pnas.210814611935914185>
- Kitous, A., & Keramidas, K. (2015). *Analysis of scenarios integrating the INDCs*. JRC policy brief, European Commission. Joint Research Centre. Retrieved from https://joint-research-centre.ec.europa.eu/publications/analysis-scenarios-integrating-indcs_en
- Kleiner, T., & Humbert, A. (2014). Numerical simulations of major ice streams in Western Dronning Maud Land, Antarctica, under wet and dry basal conditions. *Journal of Glaciology*, 60(220), 215–232. <https://doi.org/10.3189/2014JG13J006>
- Krapp, M., Robinson, A., & Ganopolski, A. (2017). SEMIC: An efficient surface energy and mass balance model applied to the Greenland ice sheet. *The Cryosphere*, 11(4), 1519–1535. <https://doi.org/10.5194/tc-11-1519-2017>
- Kravitz, B., Robock, A., Boucher, O., Schmidt, H., Taylor, K. E., Stenchikov, G., & Schulz, M. (2011). The geoengineering model intercomparison project (GeoMIP). *Atmospheric Science Letters*, 12(2), 162–167. <https://doi.org/10.1002/asl.316>

- Lee, W. R., MacMartin, D. G., Visioni, D., & Kravitz, B. (2021). High-latitude stratospheric aerosol geoengineering can be more effective if injection is limited to spring. *Geophysical Research Letters*, 48(9), e2021GL092696. <https://doi.org/10.1029/2021GL092696>
- Lee, W. R., MacMartin, D. G., Visioni, D., Kravitz, B., Chen, Y., Moore, J. C., et al. (2023). High-latitude stratospheric aerosol injection to preserve the Arctic. *Earth's Future*, 11(1), e2022EF003052. <https://doi.org/10.1029/2022EF003052>
- Lehner, F., Deser, C., Maher, N., Marotzke, J., Fischer, E. M., Brunner, L., et al. (2020). Partitioning climate projection uncertainty with multiple large ensembles and CMIP5/6. *Earth System Dynamics*, 11(2), 491–508. <https://doi.org/10.5194/esd-11-491-2020>
- LeMour, E., & Huybrechts, P. (1996). A comparison of different ways of dealing with isostasy: Examples from modeling the Antarctic ice sheet during the last glacial cycle. *Annals of Glaciology*, 23, 309–317. <https://doi.org/10.3189/S0260305500013586>
- Macias-Fauria, M., Jepson, P., Zimov, N., & Malhi, Y. (2020). Pleistocene Arctic megafaunal ecological engineering as a natural climate solution? *Philosophical Transactions of the Royal Society B*, 375(1794), 20190122. <https://doi.org/10.1098/rstb.2019.0122>
- MacMartin, D. G., Ricke, K. L., & Keith, D. W. (2018). Solar geoengineering as part of an overall strategy for meeting the 1.5°C Paris target. *Philosophical Transactions of the Royal Society A*, 376(2119), 20160454. <https://doi.org/10.1098/rsta.2016.0454>
- McMillan, M., Leeson, A. A., Shepherd, A., Briggs, K., Armitage, T., Hogg, A., et al. (2016). A high-resolution record of Greenland mass imbalance. *Geophysical Research Letters*, 43(13), 7002–7010. <https://doi.org/10.1002/2016GL069666>
- Moore, J. C., Gladstone, R., Zwinger, T., & Wolovick, M. (2018). Geoengineer polar glaciers to slow sea level rise. *Nature*, 555(7696), 303–305. <https://doi.org/10.1038/d41586-018-03036-4>
- Moore, J. C., Greve, R., Yue, C., Zwinger, T., Gillet-Chaulet, F., & Zhao, L. (2023). Dataset for “Reduced ice loss from Greenland under stratospheric aerosol injection” [Dataset]. Zenodo. <https://doi.org/10.5281/zenodo.4131582>
- Moore, J. C., Mettiäinen, I., Wolovick, M., Zhao, L., Gladstone, R., Chen, Y., et al. (2020). Targeted geoengineering: Local interventions with global implications. *Global Policy*, 12(S1), 108–118. <https://doi.org/10.1111/1758-5899.12867>
- Moore, J. C., Yue, C., Zhao, L., Guo, X., Watanabe, S., & Ji, D. (2019). Greenland ice sheet response to stratospheric aerosol injection geoengineering. *Earth's Future*, 7(12), 1451–1463. <https://doi.org/10.1029/2019EF001393>
- Morlighem, M., Rignot, E., Mougino, J., Seroussi, H., & Larour, E. (2014). Deeply incised submarine glacial valleys beneath the Greenland ice sheet. *Nature Geoscience*, 7(6), 418–422. <https://doi.org/10.1038/ngeo2167>
- Morlighem, M., Williams, C. N., Rignot, E., An, L., Arndt, J. E., Bamber, J. L., et al. (2017). BedMachine v3: Complete bed topography and ocean bathymetry mapping of Greenland from multi-beam echo sounding combined with mass conservation. *Geophysical Research Letters*, 44(21), 11051–11061. <https://doi.org/10.1002/2017GL074954>
- Mougino, J., Rignot, E., Björk, A. A., van den Broeke, M., Millan, R., Morlighem, M., et al. (2019). Forty-six years of Greenland Ice Sheet mass balance from 1972 to 2018. *Proceedings of the National Academy of Sciences of the United States of America*, 116(19), 9239–9244. <https://doi.org/10.1073/pnas.1904242116>
- Niemeier, U., & Timmreck, C. (2015). What is the limit of stratospheric sulfur climate engineering? *Atmospheric Chemistry and Physics*, 15(16), 9129–9141. <https://doi.org/10.5194/acp-15-9129-2015>
- Nowicki, S., Goelzer, H., Seroussi, H., Payne, A. J., Lipscomb, W. H., Abe-Ouchi, A., et al. (2020). Experimental protocol for sea level projections from ISMIP6 stand-alone ice sheet models. *The Cryosphere*, 14(7), 2331–2368. <https://doi.org/10.5194/tc-14-2331-2020>
- Nowicki, S. M. J., Payne, A., Larour, E., Seroussi, H., Goelzer, H., Lipscomb, W., et al. (2016). Ice sheet model intercomparison project (ISMIP6) contribution to CMIP6. *Geoscientific Model Development*, 9(12), 4521–4545. <https://doi.org/10.5194/gmd-9-4521-2016>
- Oppenheimer, M., Little, C. M., & Cooke, R. M. (2016). Expert judgement and uncertainty quantification for climate change. *Nature Climate Change*, 6(5), 445–451. <https://doi.org/10.1038/nclimate2959>
- Pattyn, F., Ritz, C., Hanna, E., Asay-Davis, X., DeConto, R., Durand, G., et al. (2018). The Greenland and Antarctic ice sheets under 1.5°C global warming. *Nature Climate Change*, 8(12), 1053–1061. <https://doi.org/10.1038/s41558-018-0305-8>
- Rezaei, A., Karami, K., Tilmes, S., & Moore, J. C. (2022). *Changes in global teleconnection patterns under global warming and stratospheric aerosol intervention scenarios*. EGU sphere. <https://doi.org/10.5194/egusphere-2022-974>
- Rückamp, M., Falk, U., Frieler, K., Lange, S., & Humbert, A. (2018). The effect of overshooting 1.5°C global warming on the mass loss of the Greenland ice sheet. *Earth System Dynamics*, 9(4), 1169–1189. <https://doi.org/10.5194/esd-9-1169-2018>
- Schlund, M., Lauer, A., Gentile, P., Sherwood, S. C., & Eyring, V. (2020). Emergent constraints on equilibrium climate sensitivity in CMIP5: Do they hold for CMIP6? *Earth System Dynamics*, 11(4), 1233–1258. <https://doi.org/10.5194/esd-11-1233-2020>
- SICOPOLIS Authors. (2022). SICOPOLIS (version 5-dev, branch develop, revision 62baf9e6d) [Software]. Zenodo. <https://doi.org/10.5281/zenodo.8084818>
- Simmons, A. (2006). ERA-Interim: New ECMWF reanalysis products from 1989 onwards. *ECMWF Newsletter*, 110, 25–35. <https://doi.org/10.21957/pocnex23c6>
- Slater, A. G., Pitman, A. J., & Desborough, C. E. (1998). The validation of a snow parameterization designed for use in general circulation models. *International Journal of Climatology*, 18(6), 595–617. [https://doi.org/10.1002/\(SICI\)1097-0088\(199805\)18:6<595::AID-JOC275>3.0.CO;2-O](https://doi.org/10.1002/(SICI)1097-0088(199805)18:6<595::AID-JOC275>3.0.CO;2-O)
- Slater, D. A., Felikson, D., Straneo, F., Goelzer, H., Little, C. M., Morlighem, M., et al. (2020). Twenty-first century ocean forcing of the Greenland ice sheet for modelling of sea level contribution. *The Cryosphere*, 14(3), 985–1008. <https://doi.org/10.5194/tc-2019-222>
- Slater, D. A., Straneo, F., Felikson, D., Little, C. M., Goelzer, H., Fettweis, X., & Holte, J. (2019). Estimating Greenland tidewater glacier retreat driven by submarine melting. *The Cryosphere*, 13(9), 2489–2509. <https://doi.org/10.5194/tc-13-2489-2019>
- Smith, W., & Wagner, G. (2018). Stratospheric aerosol injection tactics and costs in the first 15 years of deployment. *Environmental Research Letters*, 13(12), 124001. <https://doi.org/10.1088/1748-9326/aae98d>
- Tilmes, S., Richter, J. H., Kravitz, B., MacMartin, D. G., Mills, M. J., Simpson, I. R., et al. (2018). CESM1(WACCM) stratospheric aerosol geoengineering large ensemble project. *Bulletin of the American Meteorological Society*, 99(11), 2361–2371. <https://doi.org/10.1175/BAMS-D-17-0267.1>
- Trusel, L. D., Frey, K. E., Das, S. B., Karnauskas, K. B., Kuipers Munneke, P., van Meijgaard, E., & van den Broeke, M. R. (2015). Divergent trajectories of Antarctic surface melt under two twenty-first-century climate scenarios. *Nature Geoscience*, 8(12), 927–932. <https://doi.org/10.1038/ngeo2563>
- Van de Berg, W. J., Van Den Broeke, M., Ettema, J., Van Meijgaard, E., & Kaspar, F. (2011). Significant contribution of insolation to Eemian melting of the Greenland ice sheet. *Nature Geoscience*, 4(10), 679–683. <https://doi.org/10.1038/NGEO1245>
- Van den Broeke, M., Bamber, J. L., Ettema, J., Rignot, E., Schrama, E., van de Berg, W. J., et al. (2009). Partitioning recent Greenland mass loss. *Science*, 326(5955), 984–986. <https://doi.org/10.1126/science.1178176>
- Vaughan, N. E., & Lenton, T. M. (2011). A review of climate geoengineering proposals. *Climatic Change*, 109(3–4), 745–790. <https://doi.org/10.1007/s10584-011-0027-7>
- Visioni, D., Kravitz, B., Robock, A., Tilmes, S., Haywood, J. M., Boucher, O., et al. (2023). Opinion: The scientific and community-building roles of the geoengineering model intercomparison project (GeoMIP) – Past, present, and future. *Atmospheric Chemistry and Physics*, 23(9), 5149–5176. <https://doi.org/10.5194/acp-23-5149-2023>

- Visioni, D., MacMartin, D. G., Kravitz, B., Lee, W., Simpson, I. R., & Richter, J. H. (2020). Reduced poleward transport due to stratospheric heating under stratospheric aerosols geoengineering. *Geophysical Research Letters*, *47*(17), e2020GL089470. <https://doi.org/10.1029/2020GL089470>
- Wang, W., He, C., Moore, J. C., Wang, G., & Niu, G.-Y. (2022). Physics-based narrowband optical parameters for snow albedo simulation in climate models. *Journal of Advances in Modeling Earth Systems*, *14*(1), e2020MS002431. <https://doi.org/10.1029/2020MS002431>
- Watanabe, S., Hajima, T., Sudo, K., Nagashima, T., Takemura, T., Okajima, H., et al. (2011). MIROC-ESM 2010: Model description and basic results of CMIP5-20c3m experiments. *Geoscientific Model Development*, *4*, 845–872. <https://doi.org/10.5194/gmd-4-845-2011>
- Xie, M., Moore, J. C., Zhao, L., Wolovick, M., & Muri, H. (2022). Impacts of three types of solar geoengineering on the Atlantic meridional overturning circulation. *Atmospheric Chemistry and Physics*, *22*(7), 4581–4597. <https://doi.org/10.5194/acp-22-4581-2022>
- Yue, C., Steffensen Schmidt, L., Zhao, L., Wolovick, M., & Moore, J. C. (2021). Vatnajökull mass loss under solar geoengineering due to the North Atlantic meridional overturning circulation. *Earth's Future*, *9*(9), e2021EF002052. <https://doi.org/10.1029/2021EF002052>
- Zwally, H. J., Giovinetto, M. B., Beckley, M. A., & Saba, J. L. (2012). *Antarctic and Greenland drainage systems*. GSFC Cryospheric Sciences Laboratory. Retrieved from <https://earth.gsfc.nasa.gov/cryo/data/polar-altimetry/antarctic-and-greenland-drainage-systems>